

NACA TN 3948

# NATIONAL ADVISORY COMMITTEE FOR AERONAUTICS

TECHNICAL NOTE 3948

PRELIMINARY DATA AT A MACH NUMBER OF 2.40 OF  
THE CHARACTERISTICS OF FLAP-TYPE CONTROLS  
EQUIPPED WITH PLAIN OVERHANG BALANCES

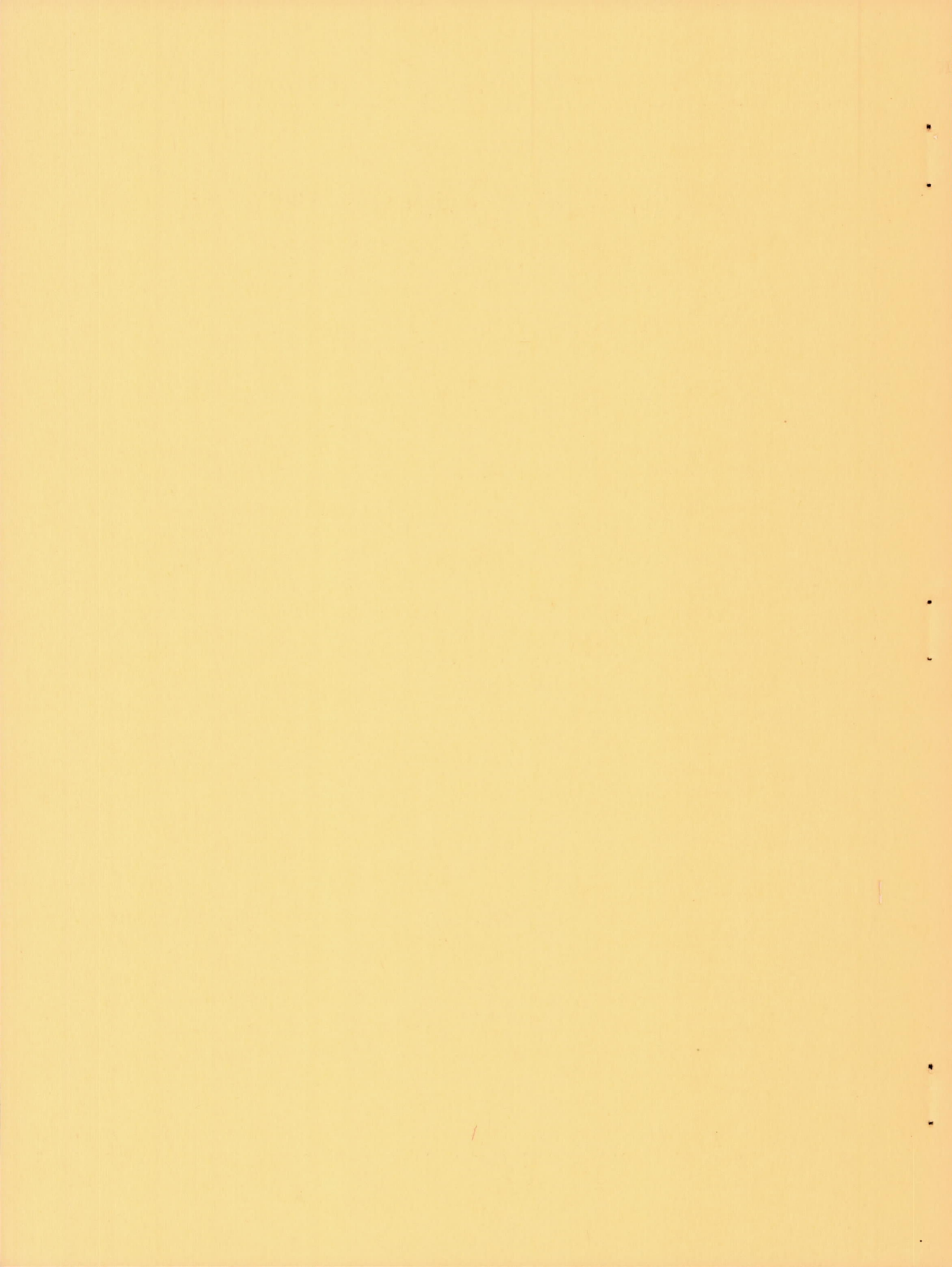
By James N. Mueller and K. R. Czarnecki

Langley Aeronautical Laboratory  
Langley Field, Va.



Washington

March 1957



---

TECHNICAL NOTE 3948

---

PRELIMINARY DATA AT A MACH NUMBER OF 2.40 OF  
THE CHARACTERISTICS OF FLAP-TYPE CONTROLS  
EQUIPPED WITH PLAIN OVERHANG BALANCES<sup>1</sup>

By James N. Mueller and K. R. Czarnecki

SUMMARY

An investigation has been made at a Mach number of 2.40 to determine the aerodynamic characteristics of plain overhang balances on flap-type controls. The tests were made on an essentially two-dimensional wing in conjunction with three trailing-edge flaps having balance lengths of 38, 60, and 82 percent of the flap chord. The effect of wing-flap gap size was investigated for the flap with the 38-percent balance.

A preliminary analysis of the data indicated that the 38-percent balance was ineffective because of its location close behind the bluff base of the rearward part of the wing section. When the balance chord was increased from 38 percent to 82 percent of the flap chord, an appreciable balancing effect was obtained. There was a small loss of lift with increase in aerodynamic balance. The effect of increasing wing-flap gap size was to improve the lift, to alleviate the magnitude and extent of the breaks in the curves of the hinge-moment, pitching-moment, and normal-force coefficients, and, in general, to increase the chord force of the wing-flap combination.

INTRODUCTION

The high hinge moments associated with control surfaces of vehicles flying at supersonic speeds are currently of paramount concern. It is desirable to reduce or balance these hinge moments through use of some form of aerodynamic balance. At present, adequate theory is not yet available for predicting balancing characteristics and experimental studies are far too meager to supply the required information. An

---

<sup>1</sup>Supersedes recently declassified NACA Research Memorandum L52F10 by James N. Mueller and K. R. Czarnecki, 1952.



investigation, therefore, is being made in the Langley 9-inch supersonic tunnel to determine the balancing characteristics of plain overhang balances on flap-type controls. These studies are made in a two-dimensional flow field by means of pressure distributions rather than force tests in order to determine the nature of the flow fields about the wing.

Tests have been completed at a Mach number of 2.40 for an essentially two-dimensional 6-percent wing equipped with trailing-edge flaps of varying aerodynamic balance. These flaps had diamond-shaped sections with sharp leading and trailing edges and represented 30 percent of the model chord. Aerodynamic balances of 38, 60, and 82 percent were used with the location of the flap maximum thickness coinciding with the hinge line. The gap-model chord ratios were 0.033 and 0.083 and the Reynolds number of the tests was  $0.78 \times 10^6$ . In order to expedite the publication of the data, the results of the investigation are presented with only preliminary analyses.

#### SYMBOLS

$p_l$	local static pressure
$p$	stream static pressure
$M$	stream Mach number
$\gamma$	ratio of specific heats for air (1.4)
$q$	stream dynamic pressure, $\frac{\gamma}{2} M^2 p$
$P$	pressure coefficient, $\frac{p_l - p}{q}$
$c_f$	flap chord back of hinge line
$c_b$	chord of balance forward of hinge line
$c_t$	total flap chord, $c_b + c_f$
$c$	model chord, main wing plus flap and exclusive of gap



n	section normal force, positive upward
m	section pitching moment about midchord, positive when it tends to rotate the leading edge of airfoil upward
h	section hinge moment of flap, positive when it tends to deflect trailing edge of flap downward
d	section chord force, positive rearward
$c_n$	section normal-force coefficient of complete configuration, $\frac{n}{qc}$
$c_m$	section pitching-moment coefficient of complete configuration, $\frac{m}{qc^2}$
$c_h$	section hinge-moment coefficient, $\frac{h}{qc_f^2}$
$c_h \left( \frac{c_f}{c_t} \right)^2$	section hinge-moment-coefficient parameter
$c_c$	section chord-force coefficient of complete configuration, $\frac{d}{qc}$
$\rho$	mass density of free stream
$\mu$	absolute coefficient of viscosity
V	free-stream velocity
R	Reynolds number, $\frac{\rho Vc}{\mu}$
$\alpha$	wing angle of attack
$\delta$	deflection of flap chord with respect to airfoil chord, positive when trailing edge is down
$\theta$	included angle of flap nose
$\phi$	included angle of flap trailing edge

- $\frac{x}{c}$  chordwise distance from leading edge of wing in terms of model chord, positive rearward
- $c_{h\delta}$  rate of change of flap section hinge-moment coefficient with flap deflection,  $\left(\frac{\partial c_h}{\partial \delta}\right)_\alpha$
- $c_{h\alpha}$  rate of change of flap section hinge-moment coefficient with angle of attack,  $\left(\frac{\partial c_h}{\partial \alpha}\right)_\delta$
- $c_{m\alpha}$  rate of change of pitching-moment coefficient of complete configuration with angle of attack,  $\left(\frac{\partial c_m}{\partial \alpha}\right)_\delta$

#### APPARATUS AND MODELS

The Langley 9-inch supersonic tunnel is a closed-return type of tunnel with provision for the control of the humidity and pressure. Changes in test Mach number are provided by interchangeable two-dimensional nozzle blocks forming test sections approximately 9 inches square. Eleven fine-mesh turbulence-damping screens are installed in the settling chamber ahead of the nozzles. For qualitative-flow observations, a schlieren optical system is provided. During the tests, the quantity of water vapor in the tunnel air was kept sufficiently low so that the effects of condensation in the supersonic nozzle were negligible.

Presented in figure 1 are the basic model components and their dimensions. Also illustrated is the method for coupling the flaps to the main wing. Two complete wing-flap models were used, one for measuring pressure distributions and the other for obtaining schlieren photographs. These models and their methods of installation in the tunnel are shown in figures 2 and 3, respectively. As shown in figure 1, the profile of the wing (exclusive of flap) consisted of a slab-type section with a sharp nose and a blunt trailing edge. The flaps had diamond-shaped profiles and represented values of plain overhang balance of 38, 60, and 82 percent of the flap chord back of the hinge line. The maximum thickness locations of the flaps were coincident with the hinge lines and the total flap chords were 30 percent of the chord of the wing-flap combination. The thickness ratio of the combinations was 6 percent. Variations in the wing-flap gap were obtained by translating the flap rearward from the main wing. The models were machined from steel with the sharp leading and trailing edges ground



to a thickness of less than 0.002 inch. All contours were cut to within 0.002 inch of the specified values.

### TESTS

Pressure distributions were measured on the 38, 60, and 82 percent balance wing-flap combinations with a ratio of gap to model chord of 0.033. In addition, measurements were made on the 38-percent-balance configuration with a gap-model chord ratio of 0.083.

The pressure distributions were obtained mainly at angles of attack of  $2^\circ$  and  $8^\circ$ . The flap deflections at these angles of attack usually ranged through  $\pm 20^\circ$  in increments of  $4^\circ$ . A few additional pressure distributions were made at  $\delta = 0^\circ$  and  $\delta = \pm 12^\circ$  at  $\alpha = 4^\circ, 6^\circ, \text{ and } 10^\circ$ .

All schlieren photographs were obtained with the model in profile. Generally, pictures of each wing-flap combination were made at  $\alpha = 0^\circ$  and  $\alpha = 8^\circ$  with the flap set at small ( $\delta = 0^\circ$ ), intermediate ( $\delta = \pm 11^\circ$  and  $\delta = \pm 18^\circ$ ), and large ( $\delta = \pm 25^\circ$  and  $\delta = \pm 30^\circ$ ) deflections.

The tests, including the pressure distributions and schlierens, were made at a Mach number of 2.40 and a Reynolds number of  $0.78 \times 10^6$  based on the complete model chord of 3 inches.

### PRECISION OF MEASUREMENTS

Stream surveys obtained with empty test section indicate that the mean value of the Mach number in the region occupied by the test models is 2.40 and that the variation about this mean is less than 1 percent.

Estimates of the precision of the test variables are as follows:

Hinge-moment coefficient, $c_h$ . . . . .	$\pm 0.008$
Normal-force coefficient, $c_n$ . . . . .	$\pm 0.005$
Pitching-moment coefficient, $c_m$ . . . . .	$\pm 0.002$
Chord-force coefficient, $c_c$ . . . . .	$\pm 0.004$
Angle of attack, $\alpha$ , degrees . . . . .	$\pm 0.10$
Flap angle, $\delta$ , degrees . . . . .	$\pm 0.25$
Pressure coefficient, $P$ . . . . .	$\pm 0.01$



## DISCUSSION

## Pressure Distributions

Most pressure-distribution results obtained to date are presented in figure 4. All the pressure-distribution diagrams are shown for a zero wing-flap gap condition for convenience and in order to preserve uniformity among the plots when comparisons are being made. When aerodynamic coefficients were computed the wing-flap gap however was taken into consideration. Figure 4(a) shows results obtained on the 0.38-balanced-flap model for gap-model chord ratios of 0.033 and 0.083. Figures 4(b) and 4(c) present data obtained on the 0.60- and 0.82-balanced-flap configurations, respectively, for a gap-model chord ratio of 0.033.

The theoretical pressure distributions included in figure 4 were calculated from shock-expansion theory for the case of the main wing only. No attempt was made to calculate the pressure distributions over the flap surfaces because of the complicated nature of the flows occurring in this region. Except for the regions affected by flow separations, the agreement between the theoretical and experimental pressures over the wing was generally good.

An inspection of the pressure distributions (fig. 4) for  $\alpha = 2^\circ$  reveals that, for the case of the configuration with the least amount of aerodynamic balance and 0.033 gap-chord ratio, no significant balancing pressures appear to develop on the flap balance. This apparent lack of development of any load on the flap balance is due to the fact that the well-forward location of the flap maximum thickness and the proximity of the hinge line to the wing base cause the balance to be submerged in the wake of the wing and prevent "unporting" (nose of flap rises above plane of upper wing surfaces) until the flap deflection exceeds  $19^\circ$ . (See schlieren photographs, fig. 5.) For the most part the pressure distributions back of the hinge line of the 38-percent-balance flap closely resemble those obtained on plain (or unbalanced) trailing-edge flaps.

At the higher angle of attack ( $\alpha = 8^\circ$ ) the influence of the wake from the wing is noticeably different, and the balancing effectiveness of the overhang is considerably increased. The schlieren photographs of figure 5 show that the flow separates from the upper wing surface just back of the ridge line and that the boundary of this separated region does not experience large deflections in negotiating the upper flap surface. In contrast, the flow on the lower wing surface experiences no separation and expands slightly around the wing base to impinge upon the lower balance surface of the flap. The resulting shock is seen to rise from a point ahead of the flap hinge line for all values of flap deflections. These phenomena explain the high pressure peaks on the lower flap surface forward of the hinge line shown in figure 4(a) and the



relatively small changes in the pressure distributions over the upper flap surface.

In progressing from the 0.38-balance configuration to the 0.60- and 0.82-balance configurations, the flow phenomena (fig. 5) and the pressure distributions (figs. 4(b) and 4(c)) show essentially the same trends as discussed previously. The positive pressure peaks on the lower flap surface become increasingly stronger and act upon a greater portion of the flap balance. This condition results from the rearward shift of the flap maximum thickness and hinge line so that the shock and its associated pressure rise are allowed to occur in a region more forward of the hinge line and thus to be more productive in reducing underbalance. Some improved balancing pressures at the lower values of flap deflection and angle of attack may be noted. This improvement may be attributed to the larger degree of expansion at the wing base permitted by the decreasing proximity of the flap maximum thickness.

As the amount of flap balance is increased from 0.38 to 0.82 percent, there is a corresponding loss in lift-producing effectiveness as the flap deflection approaches and exceeds the value for "unporting." This loss in lift results from the occurrence of flow separation on the main wing. (Compare pressure distributions on main wing at small and large values of  $\delta$ ; see figs. 4 and 5.)

As the gap-model chord ratio is increased from 0.033 to 0.083 (fig. 4(a)) there is usually a slight increase in negative pressure over the upper flap surface back of the hinge line. Forward of the hinge line there is a slight gain in balancing pressure on the lower flap balance surface which is characterized by small pressure peaks in the  $\pm 8^\circ$  deflection range.

An interesting feature of the pressure distributions is the total absence of any sudden, large increases in pressure at the nose of the flap as the flap nose "unports" (or rises above the plane of the upper wing surface). As seen in figure 5, this condition results from the extreme separation of the flow from the wing surface well ahead of the wing base. This separation is a direct result of the large pressure rise introduced at the gap between the wing and flap. The effects of the strong shock emanating from the point of separation show up markedly in the pressure distributions of figure 4 and cause appreciable reductions in wing lift.

#### Aerodynamic Characteristics

Effect of aerodynamic balance.- The primary data obtained from the tests were hinge moments and their variations with flap deflection and angle of attack. Other data included normal force, pitching moment,



and chord force. The parameter  $c_h \left( \frac{c_f}{c_t} \right)^2$  into which the hinge moment has been incorporated was introduced to provide a common basis for comparing the results from different flaps. All section aerodynamic coefficients were obtained from integration of the pressure diagrams.

Figures 6 and 7 show the variation of the aerodynamic characteristics of the various wing-flap configurations with flap deflection and angle of attack, respectively, for a gap-model chord ratio of 0.033.

The hinge-moment curves (fig. 6(a)) show that as the flap aerodynamic balance is increased from 38 to 82 percent the slopes of the hinge-moment curves  $c_{h\delta}$  become less negative. The change in slopes, or improvement in aerodynamic balance, is large except for the negative flap deflections at  $\alpha = 8^\circ$ . Thus the plain overhang balance tends to lose some of its balancing effectiveness ( $c_{h\delta}$ ) in a region of interest ( $\alpha$  and  $-\delta$ ) in the design of elevators. At  $\alpha = 2^\circ$  the hinge-moment curves exhibit a "break" in the region of small negative flap deflections. This break is gradually eliminated as the amount of balance is increased.

Figure 6(b), which shows normal-force characteristics, indicates that a small loss in lift occurs in the higher flap deflection range; this loss is more apparent at the low angle of attack. The occurrence of this loss in lift was previously shown to correspond to the values of flap deflection for which "unporting" was approached and exceeded. Flat spots in the curves or regions of flap ineffectiveness are evident at  $\alpha = 2^\circ$ ; at the higher angle of attack, only the least-balanced configuration exhibits a region of ineffectiveness.

Pitching-moment characteristics (fig. 6(c)) follow trends closely resembling those of the hinge-moment curves. A comparison of the values at  $\delta = 20^\circ$  shows that the pitching-moment coefficient of the 0.38 balanced-flap configuration is approximately twice that of the 0.82 balanced-flap configuration at both  $\alpha = 2^\circ$  and  $\alpha = 8^\circ$ . In the region of interest in the design of elevators,  $\alpha = 8^\circ$  and negative flap angles, the pitching-moment curves tend to converge and the changes in pitching moment due to changes in balance are small.

Chord-force coefficients (fig. 6(d)) show that generally at the low angle of attack and positive flap deflection range the least-balanced wing-flap combination has the greater chord force. At the higher angle of attack, however, the reverse is true. Also, the 60- and 82-percent balance configurations have, in general, chord forces of equal magnitudes.



Figure 7(a) shows the variation of the hinge-moment-coefficient parameter with angle of attack at constant flap deflection. The slope of the curves is relatively small, all values falling within a range of 0.001 to -0.005. It is noted that at  $\delta = 0^\circ$ , the 82-percent-balanced flap shows a very slight amount of overbalance (positive slope,  $c_{h\alpha}$ ). At  $\delta = 12^\circ$ , as the flap balance is increased from 38 percent to 82 percent, a considerable reduction in hinge moment is obtained.

Figure 7(b) presents the variation of the section normal-force coefficient with angle of attack at constant flap deflections. In general, the differences in slopes of the lift curves for the various balanced configurations and flap angles were relatively small.

Figure 7(c) shows pitching-moment characteristics of the various balanced configurations as a function of angle of attack at constant flap deflections. The values of  $c_{m\alpha}$  are relatively small, all values lying within the range of 0.0015 to -0.0055 per degree. Generally, the pitching-moment slopes become more positive as aerodynamic balance increases; this effect is more noticeable at  $\delta = 0^\circ$ .

Figure 7(d) presents chord-force-characteristics variations with angle of attack at constant flap deflections. At  $\delta = 0^\circ$  the chord-force rise with angle of attack is essentially the same for all configurations and is approximately 0.0018 per degree. At  $\delta = -12^\circ$  the chord-force rise is almost negligible. At  $\delta = 12^\circ$  the least-balanced configuration shows least chord-force rise, approximately 0.0038 per degree, as compared with 0.0048 per degree for the other configurations.

Effect of gap size.— Figures 8 and 9 show the effects of varying the gap-model chord ratio from 0.033 to 0.083 on the aerodynamic characteristics of the 38-percent-balance configuration as a function of flap deflection and angle of attack, respectively.

The principal effect of increasing gap size on the hinge moment, normal force, and pitching-moment characteristics (figs. 8(a), 8(b), and 8(c), respectively) is to alleviate the severity and extent of the breaks in the curves near  $\delta = 0^\circ$ .

Figure 8(d) shows the effect of increasing gap size on the section chord-force coefficient. For the low angles of attack, there is a slight increase in chord force associated with the increased gap size throughout the deflection range. At the higher angle of attack, a very significant increase in chord force is evident in the range of flap deflection from  $\delta \approx -8^\circ$  to  $\delta = 20^\circ$ . This increase approaches nearly 50 percent at  $\delta = 0^\circ$ . In the flap deflection range from  $\delta \approx -14^\circ$  to  $\delta = -20^\circ$  the larger size gap configuration shows least chord force.



Figure 9(a) presents the effects of gap size on the hinge-moment characteristics as a function of angle of attack at constant flap deflection. Increasing the gap size reduces the slopes of the curves approximately 30 percent at constant flap deflections of  $\delta = 0^\circ$  and  $\delta = 12^\circ$ . At a constant flap deflection of  $\delta = -12^\circ$ , the effect of increasing gap is to increase the slope of the curve approximately 22 percent.

Figure 9(b) shows the effects of gap size on the normal-force coefficients. Except for a possible small increase in slope of the normal-force-coefficient curves at  $\delta = 0^\circ$ , the effect of increasing the gap size was negligible.

The effect of gap size on pitching-moment characteristics (fig. 9(c)) is, in general, almost negligible.

The effect of increasing the gap size on the chord-force characteristics (fig. 9(d)) is to increase considerably the chord-force rise with angle of attack for the cases with the flap in the neutral position ( $\delta = 0^\circ$ ) and at  $\delta = 12^\circ$ . The former case shows a chord-force-rise increase over that of the smaller gap of approximately 30 percent whereas the latter shows about 17 percent. At  $\delta = -12^\circ$ , there is a slight increase in chord-force coefficients with increase in gap; however, the chord-force rise with angle of attack is approximately the same for both gap sizes.

## CONCLUSIONS

Preliminary analysis of the results of tests made at a Mach number of 2.40 and a Reynolds number of  $0.78 \times 10^6$  to determine the balancing characteristics of plain overhang balances on flap-type controls have indicated the following conclusions:

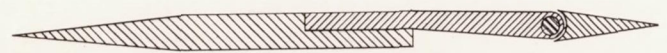
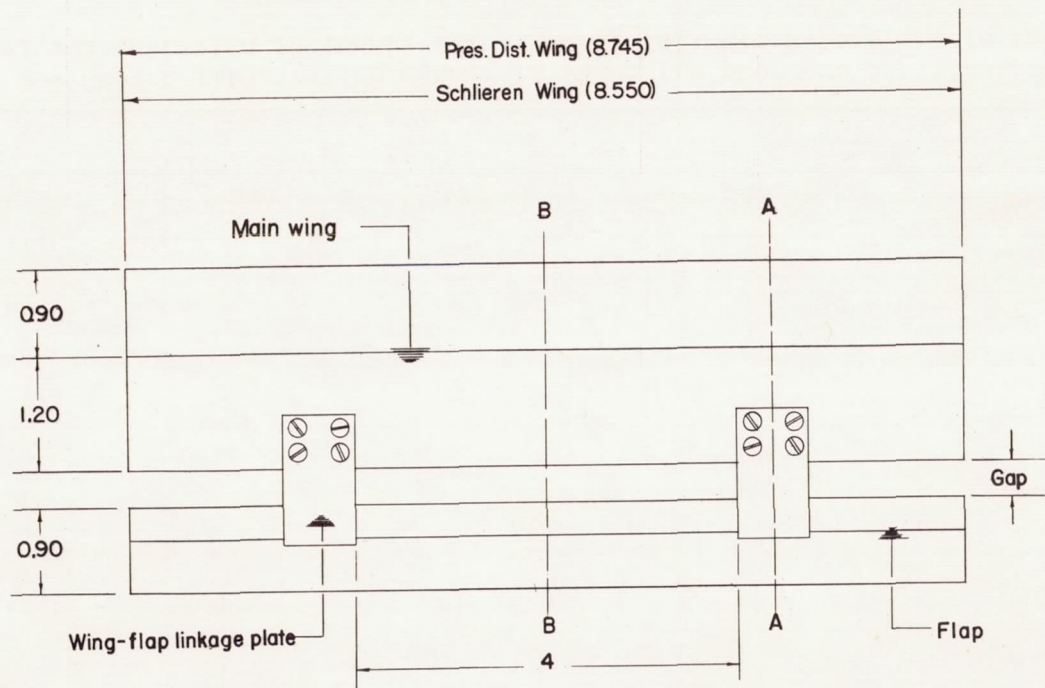
1. The 38-percent balance was ineffective because of its location close behind the bluff base of the rearward part of the wing section. However, as the balance chord was increased to 82 percent of the flap chord, an appreciable balancing effect was obtained resulting in a rate of change of flap section hinge-moment coefficient with flap deflection  $c_{h\delta}$  of about -0.004. The corresponding rate of change of flap section hinge-moment coefficient with angle of attack  $c_{h\alpha}$  was approximately zero.

2. A small loss in lift occurred with increase in aerodynamic balance. This loss was found to correspond to the values of flap deflection for which "unporting" (nose of flap rising above plane of upper wing surfaces) was approached and exceeded.

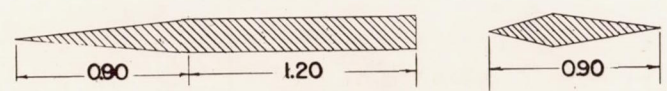
3. The effect of increasing the gap-model chord ratio from 0.033 to 0.083 on the 38-percent-balanced configuration was to improve the lift, to alleviate the magnitude and extent of the breaks in the hinge-moment, pitching-moment, and normal-force coefficient curves, and, in general, to increase the chord force of the wing-flap combination.

Langley Aeronautical Laboratory,  
National Advisory Committee for Aeronautics,  
Langley Field, Va., June 10, 1952.





Section A-A



Section B-B

Flap	$C_{p, f}$	$\theta/2$	$\phi/2$	Gap	Hinge line at $(x/c)_{Gap=0}$
	0.38	19.00°	78.5°	0.100 0.250	0.783
	0.60	14.93°	9.09°	0.100	0.816
	0.82	12.53°	10.31°	0.100	0.835

Figure 1.- General arrangements and basic dimensions of the pressure distribution and schlieren models. All dimensions are in inches.

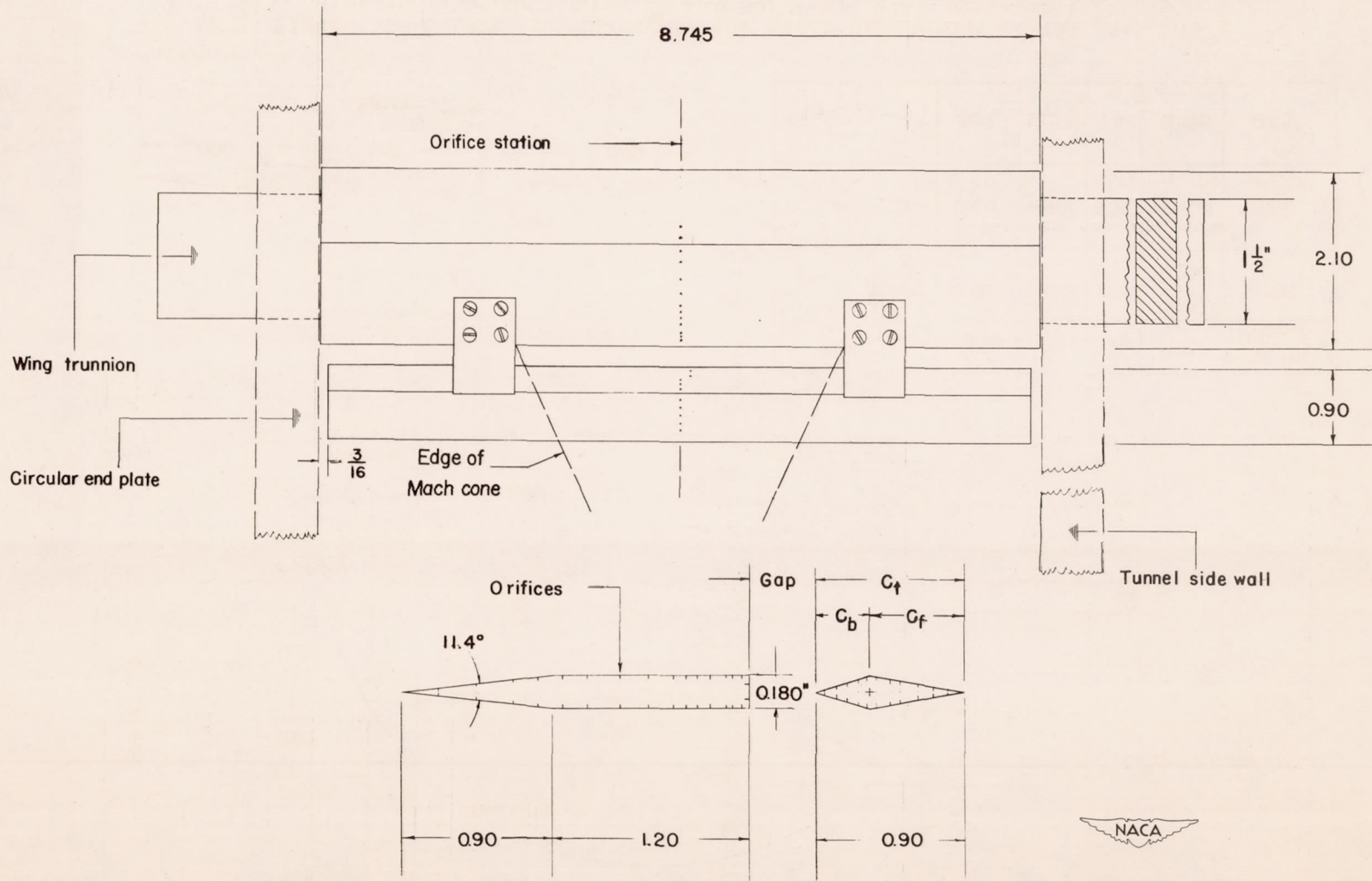


Figure 2.- Sketch illustrating manner in which the pressure distribution model was installed in tunnel for testing. All dimensions are in inches.

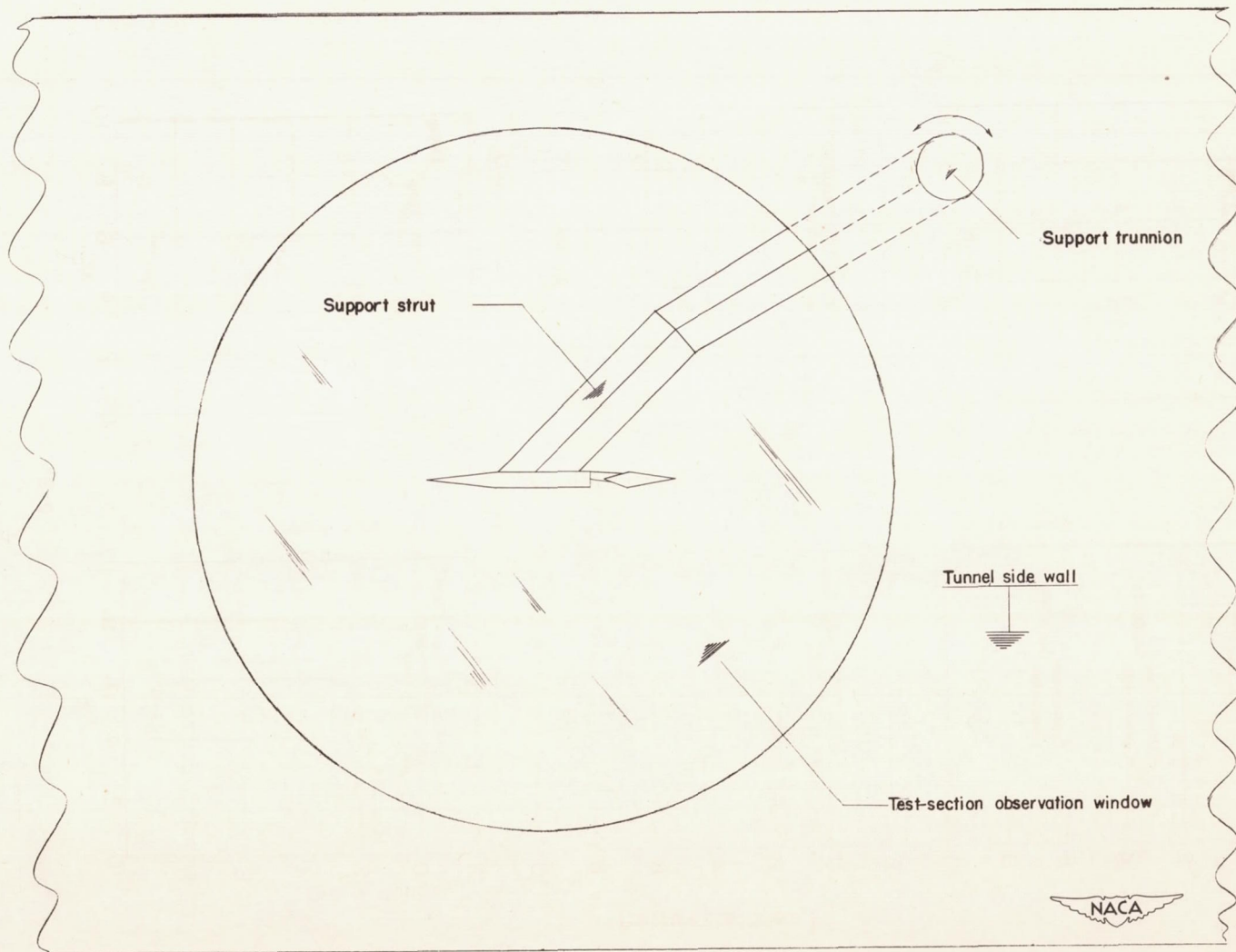
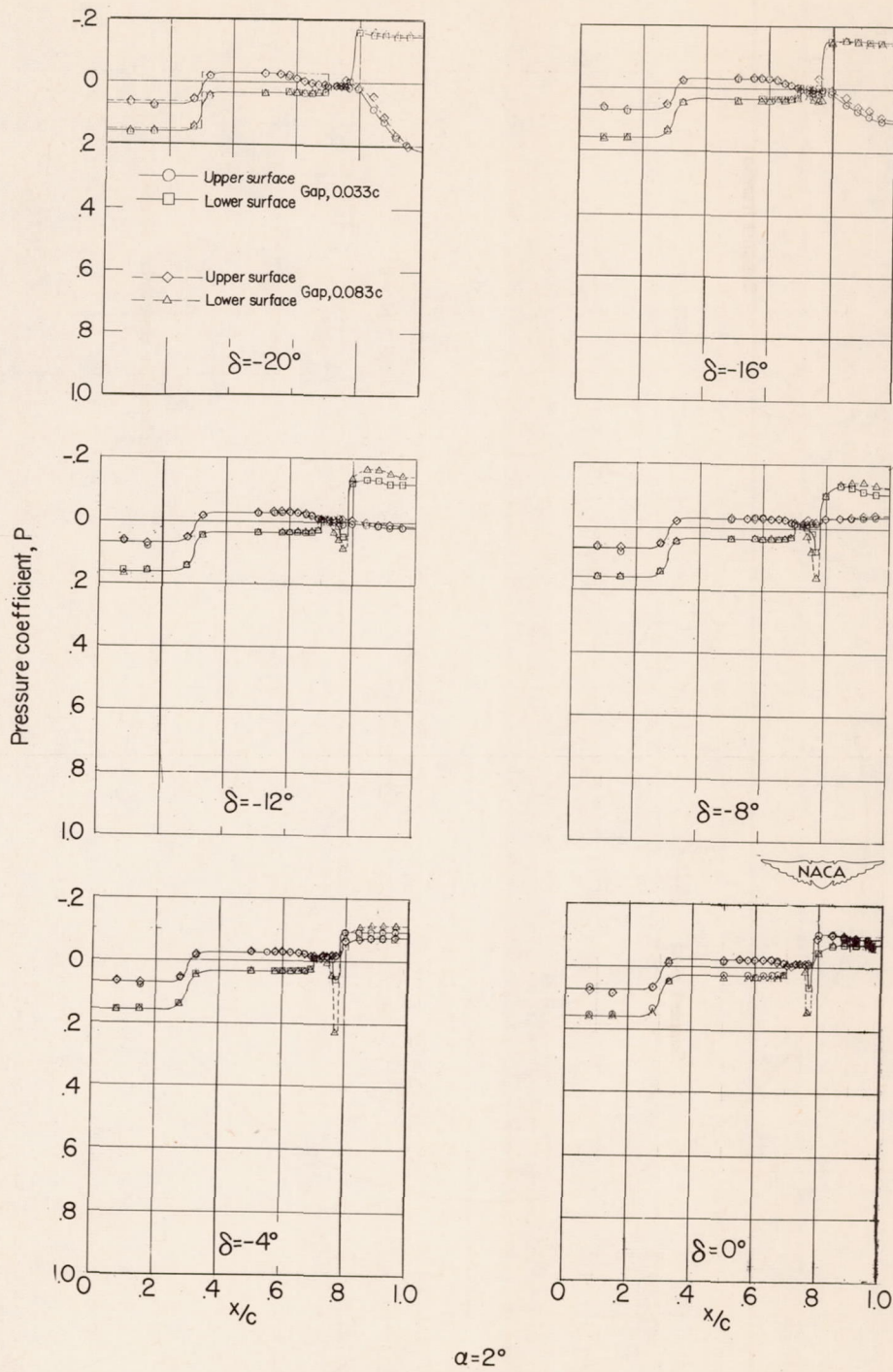


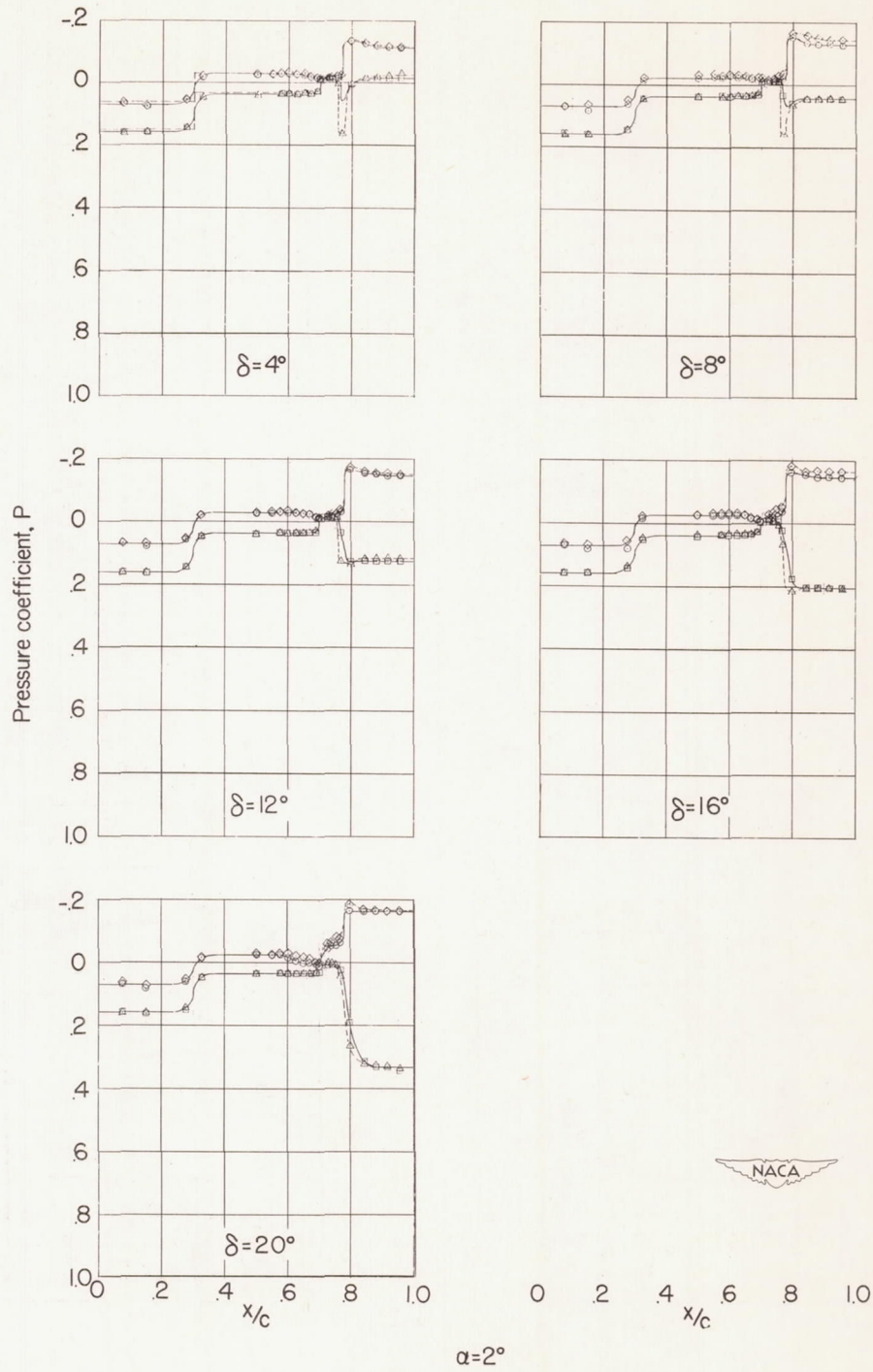
Figure 3.- Sketch showing method of mounting schlieren model for visual-flow observations.





(a)  $\frac{c_b}{c_f} = 0.38.$

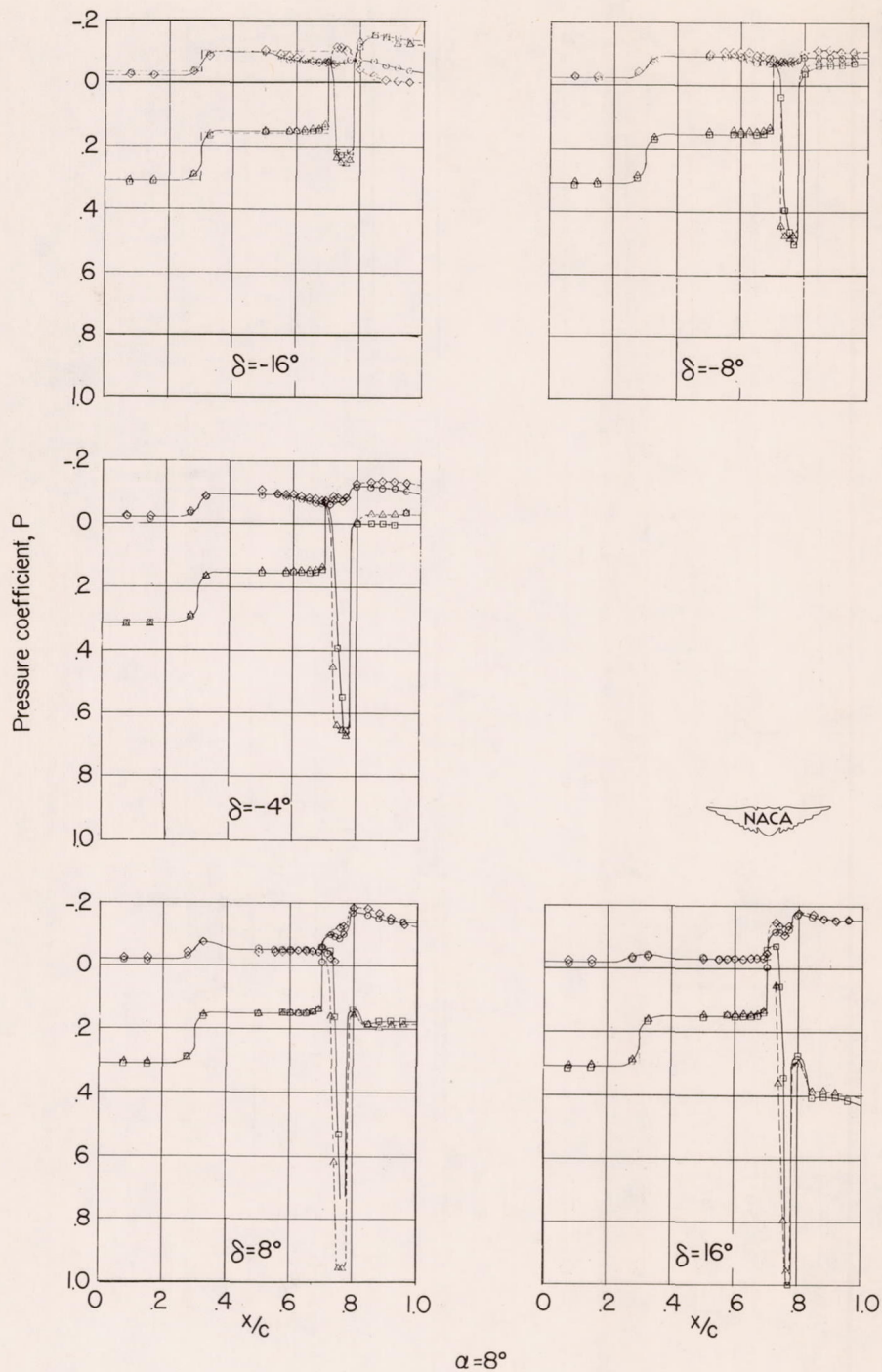
Figure 4.- Typical pressure distributions over a 6-percent-thick symmetrical wing equipped with trailing-edge flap having various amounts of aerodynamic balance.  $M = 2.40$ ;  $R = 0.78 \times 10^6$ . (Actual gap not shown.)



(a) Continued.

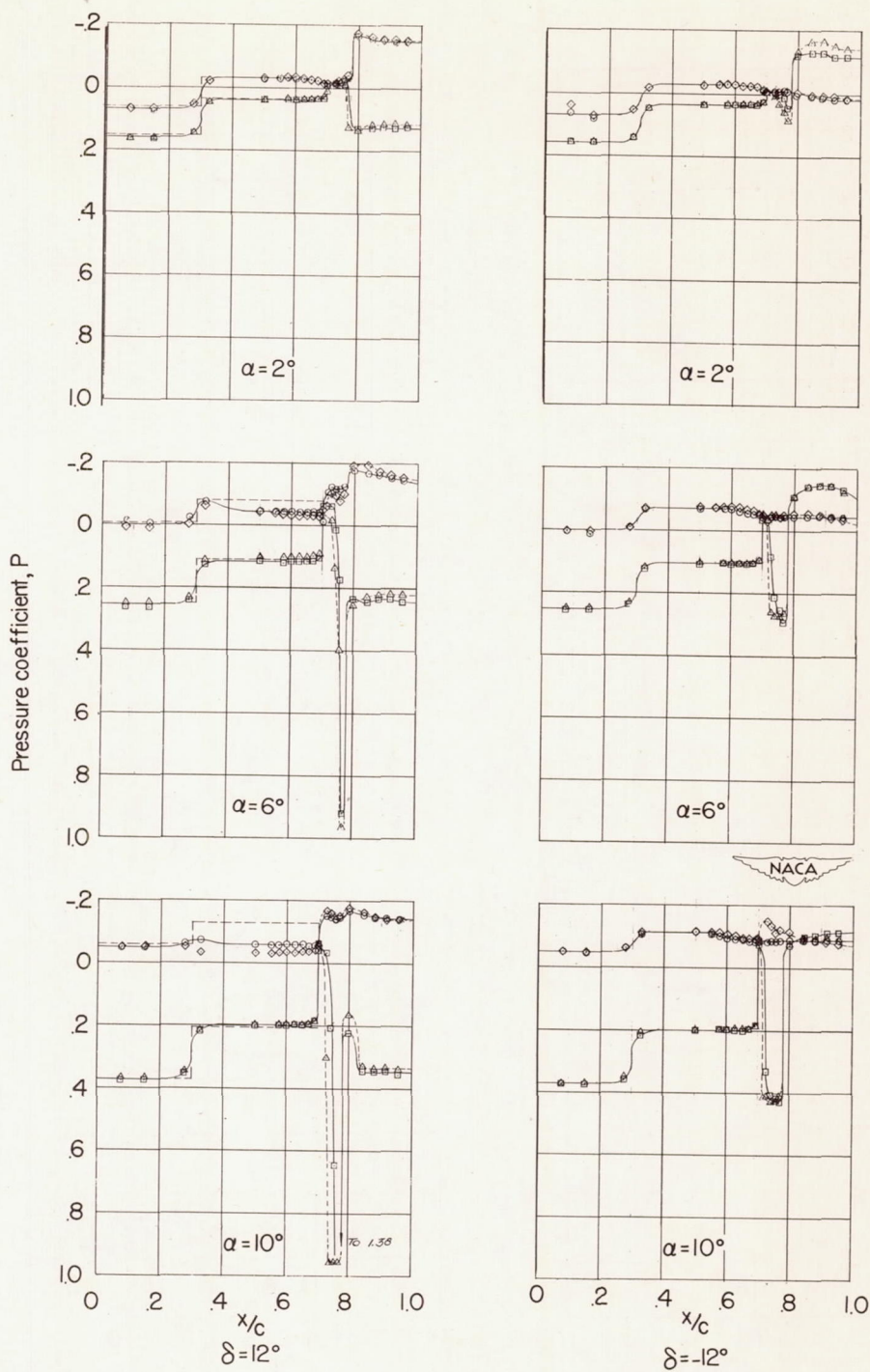
Figure 4.- Continued.





(a) Continued.

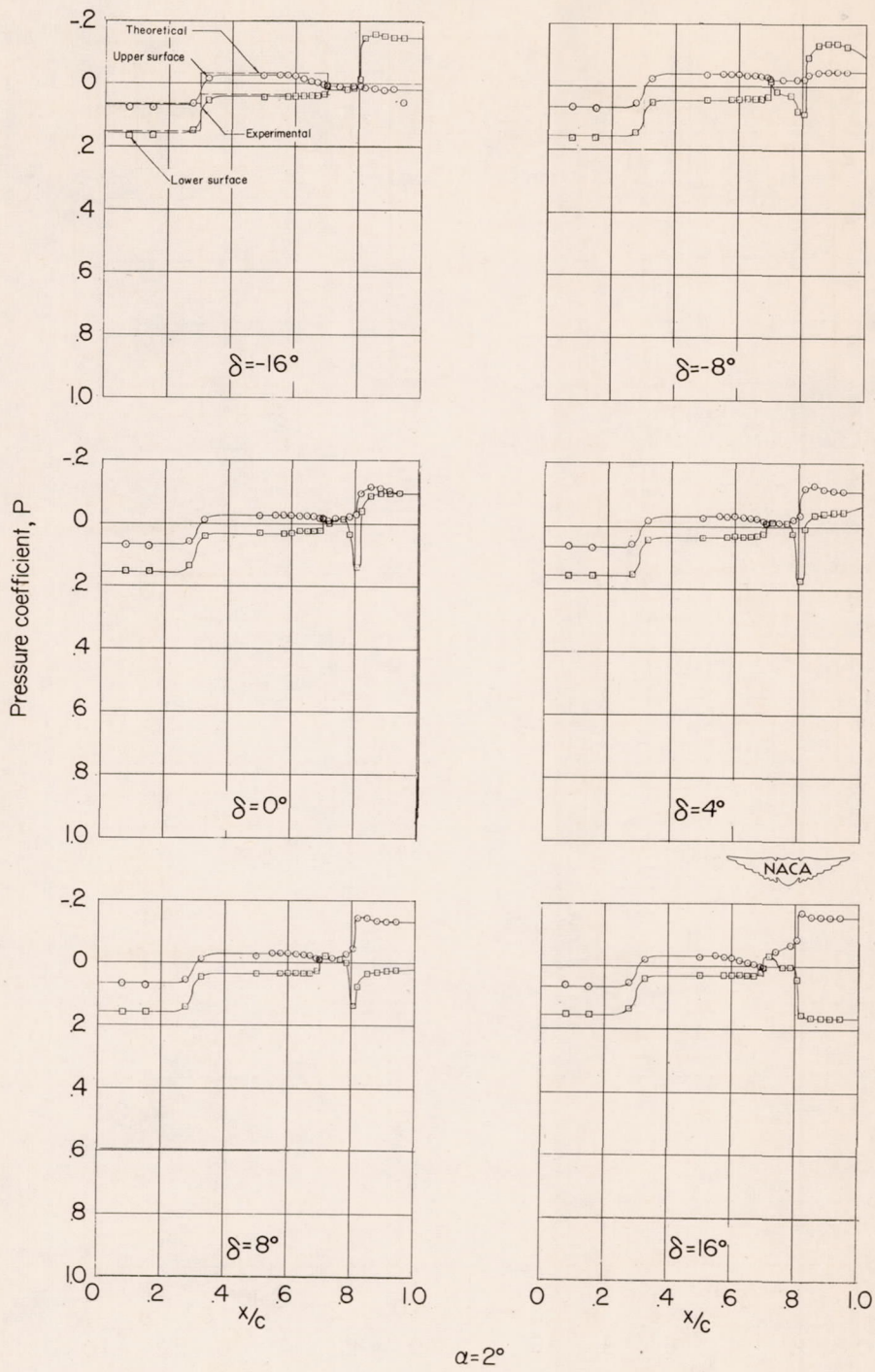
Figure 4.- Continued.



(a) Concluded.

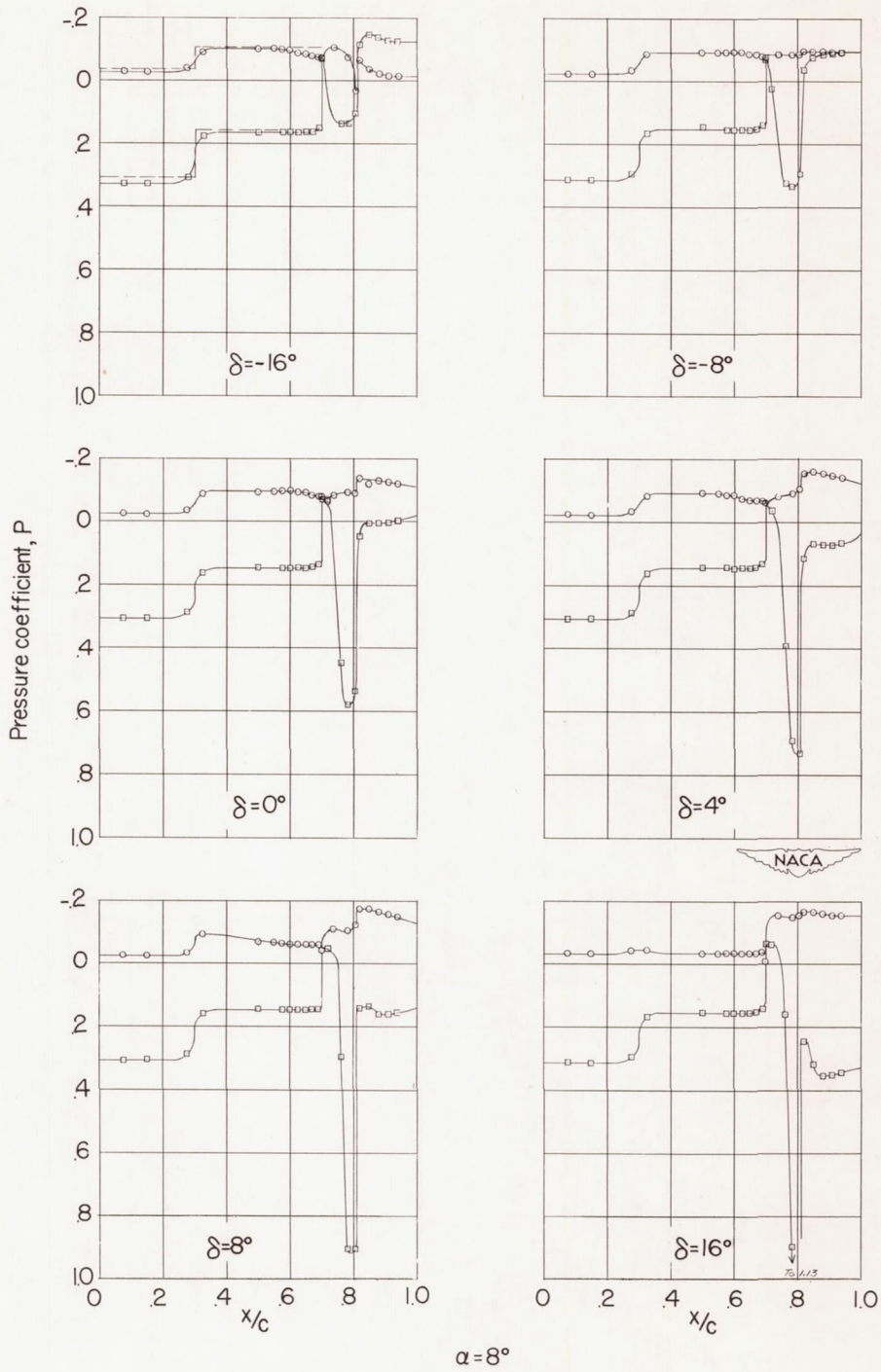
Figure 4.- Continued.





(b)  $\frac{c_b}{c_f} = 0.60.$

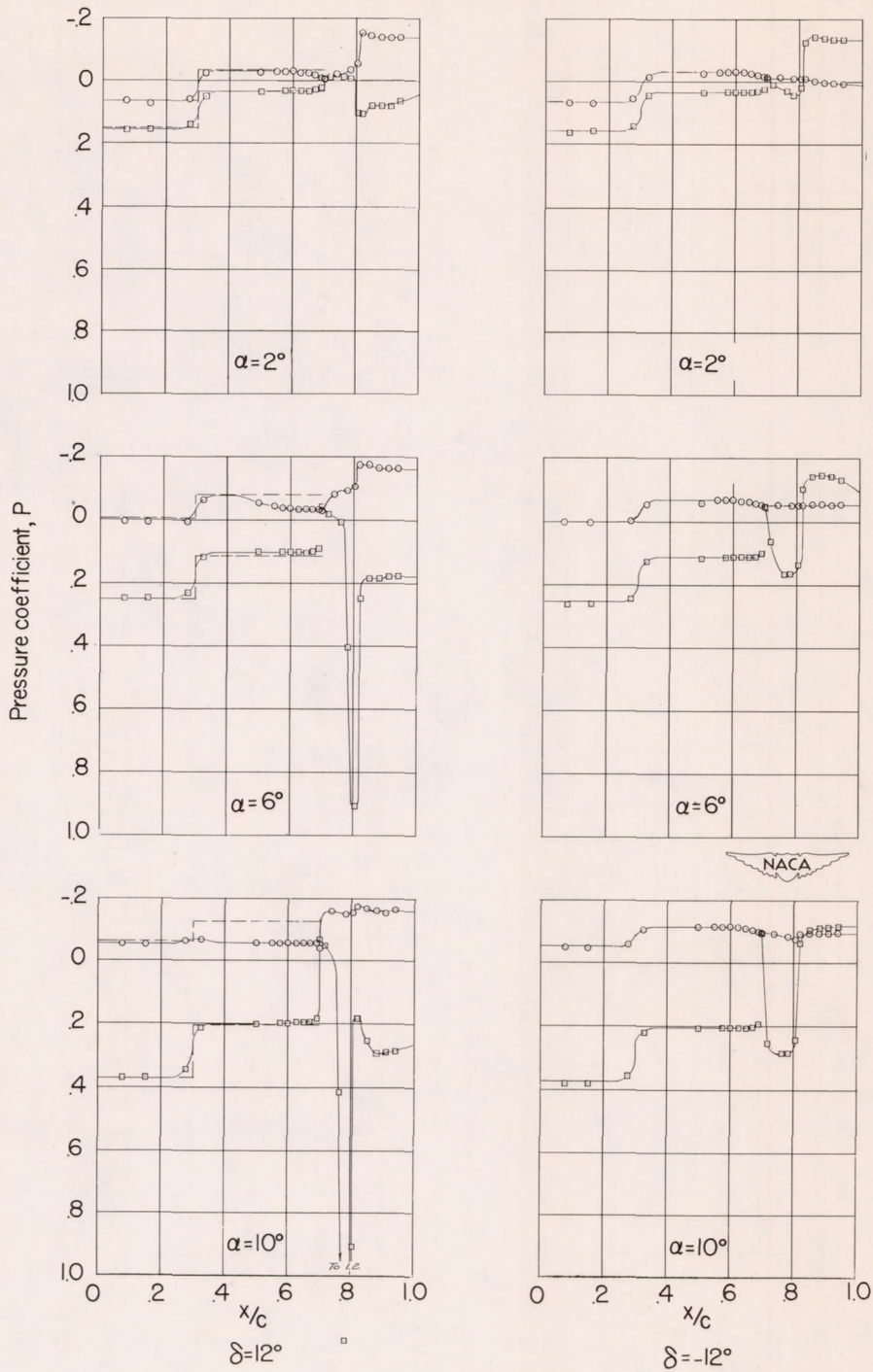
Figure 4.- Continued.



(b) Continued.

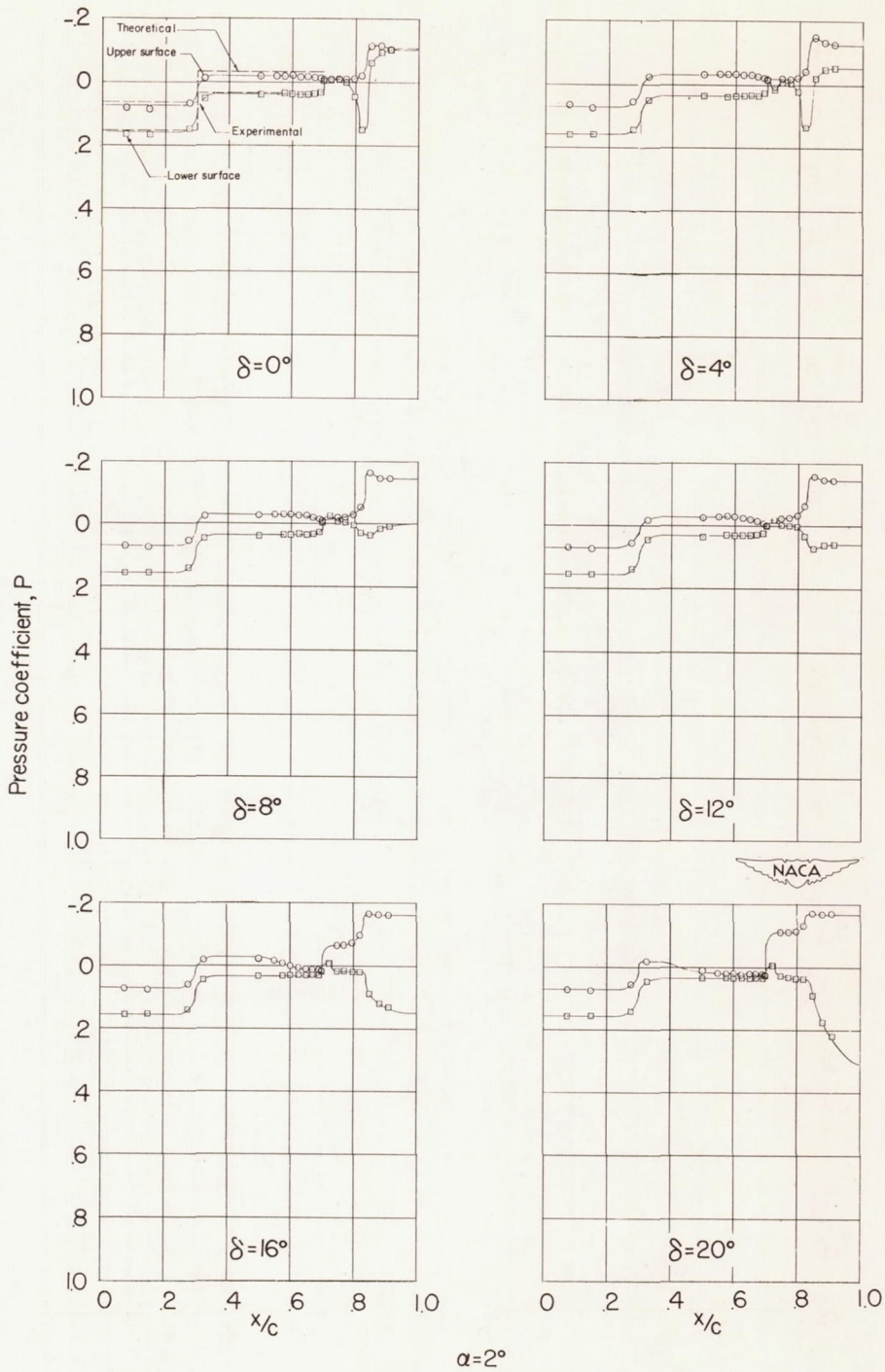
Figure 4.- Continued.





(b) Concluded.

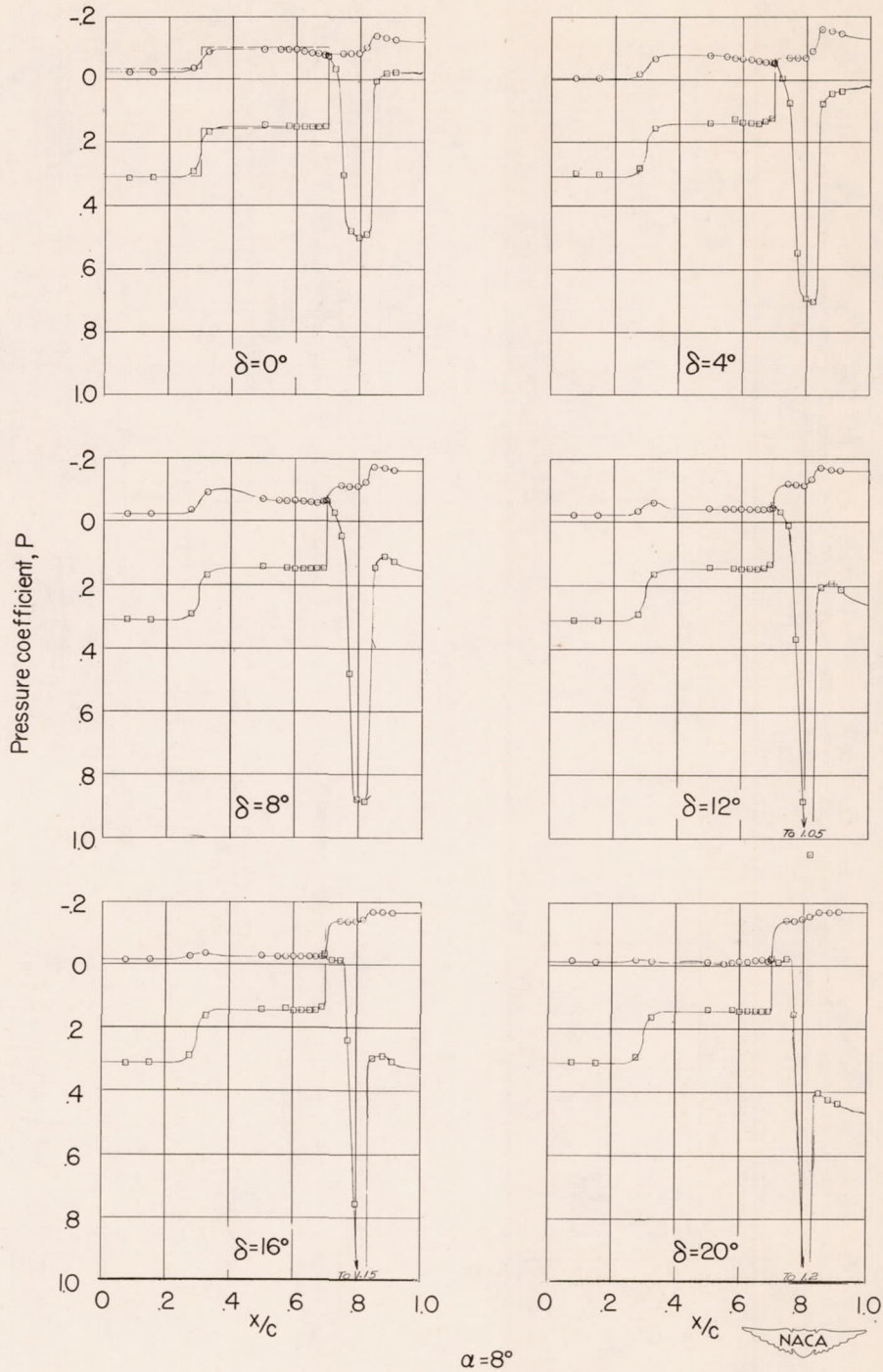
Figure 4.- Continued.



(c)  $\frac{c_b}{c_f} = 0.82.$

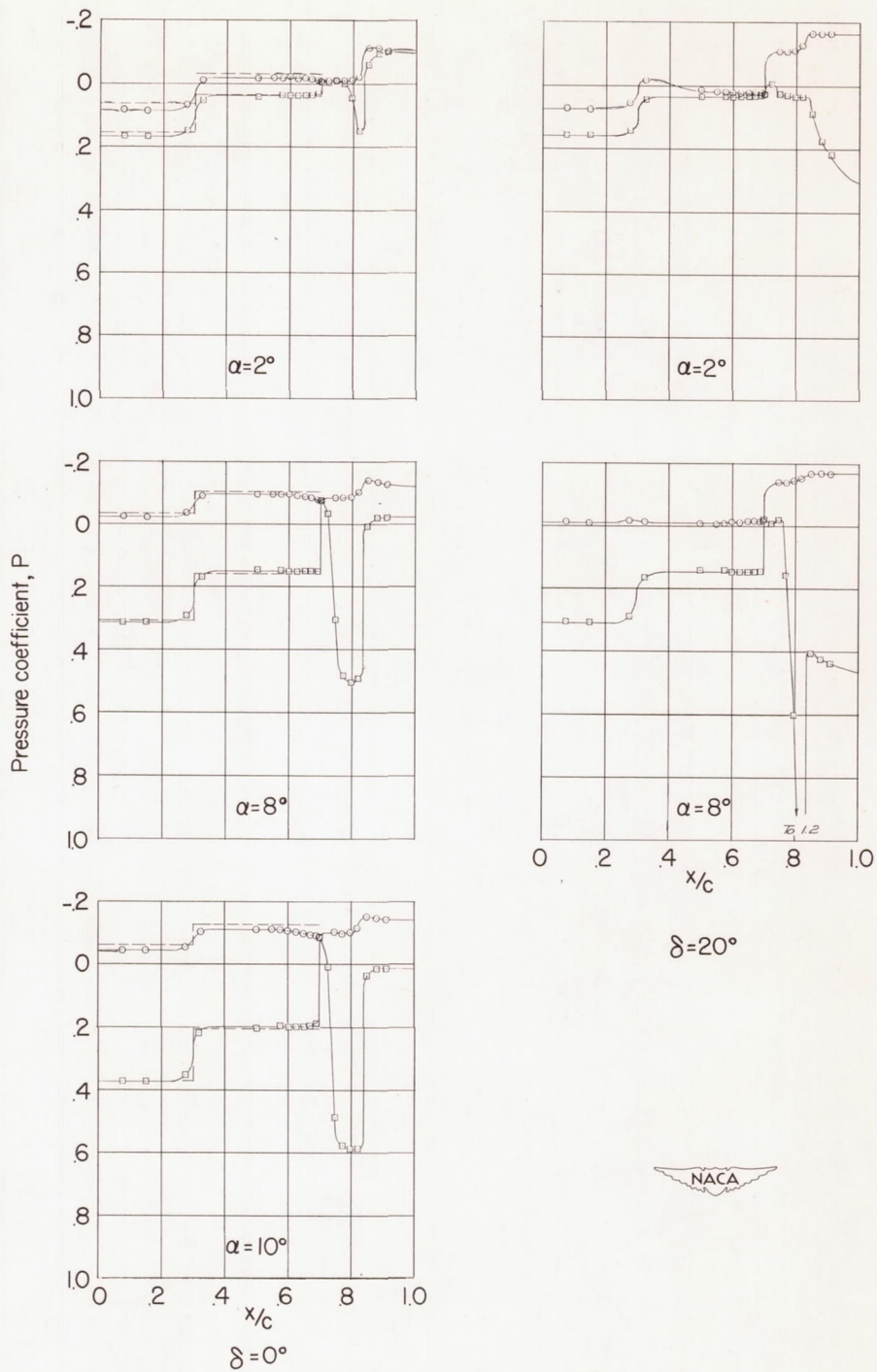
Figure 4.- Continued.





(c) Continued.

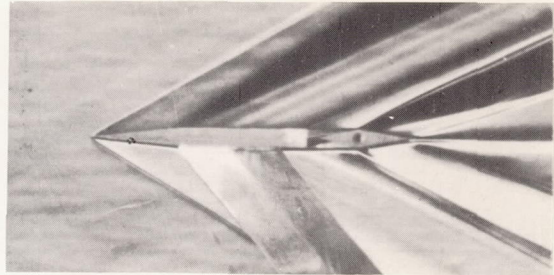
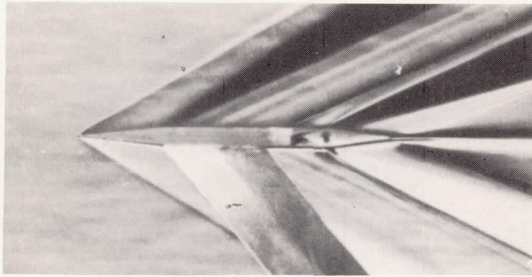
Figure 4.- Continued.



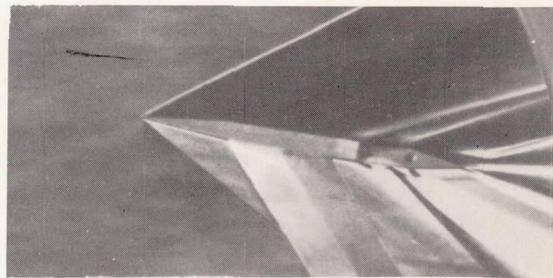
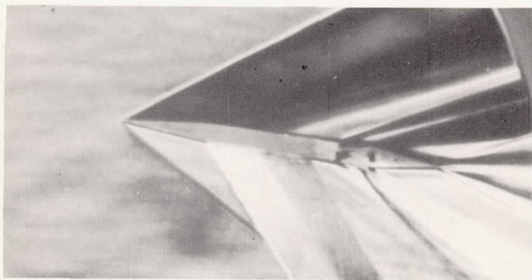
(c) Concluded.

Figure 4.- Concluded.

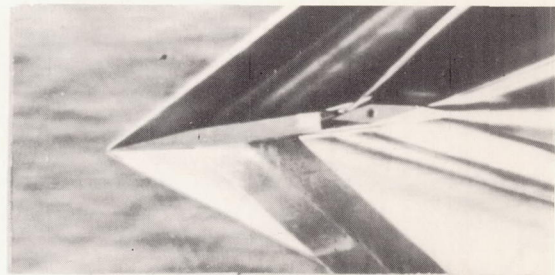
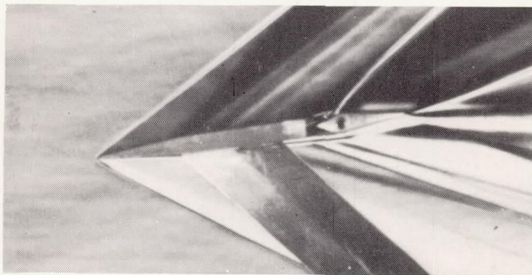




$\alpha = 0^\circ, \delta = 0^\circ$



$\alpha = 8^\circ, \delta = 0^\circ$



$\alpha = -8^\circ, \delta = 0^\circ$

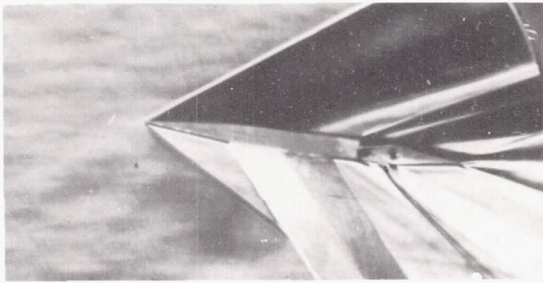


L-75139

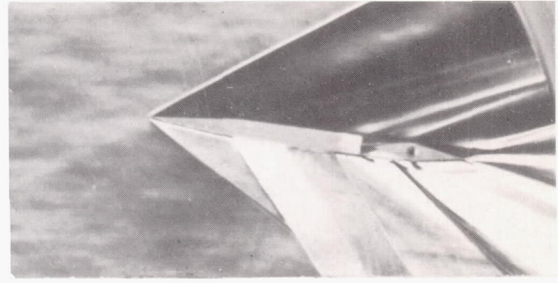
$$\frac{c_b}{c_f} = 0.38$$

$$\frac{c_b}{c_f} = 0.82$$

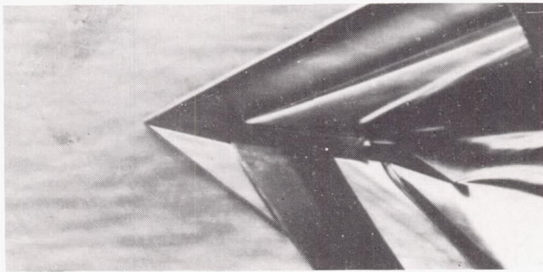
Figure 5.- Schlieren pictures of flow about 6-percent-thick symmetrical wing equipped with trailing-edge flaps having aerodynamic balances of 38 and 82 percent. Wing-flap gap,  $0.033c$ ;  $M = 2.40$ ;  $R = 0.78 \times 10^6$ .



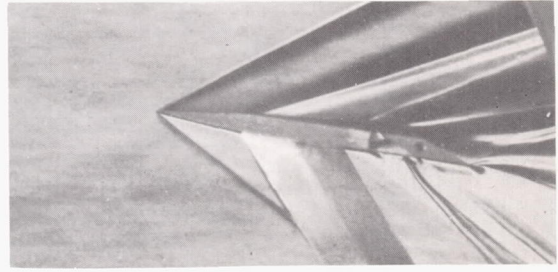
$$\alpha = 8^\circ, \delta = 0^\circ$$



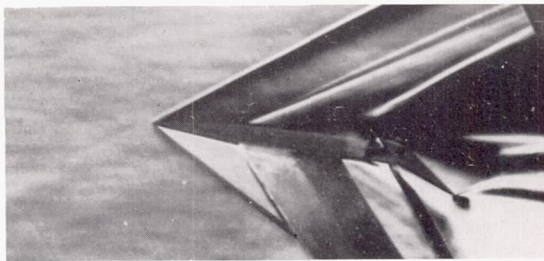
$$\alpha = 8^\circ, \delta = 0^\circ$$



$$\alpha = 8^\circ, \delta = 18^\circ$$

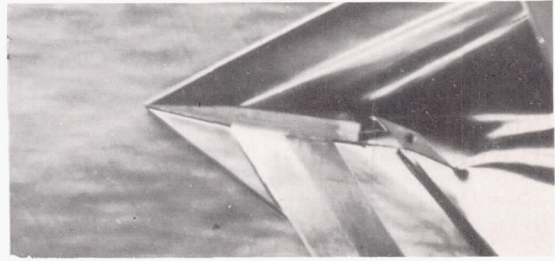


$$\alpha = 8^\circ, \delta = 11^\circ$$



$$\alpha = 8^\circ, \delta = 30^\circ$$

$$\frac{c_b}{c_f} = 0.38$$



$$\alpha = 8^\circ, \delta = 25^\circ$$

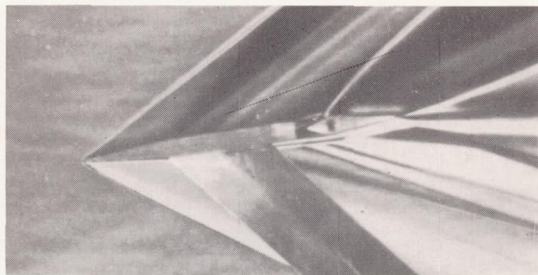
$$\frac{c_b}{c_f} = 0.82$$

Figure 5.- Continued.



L-75140

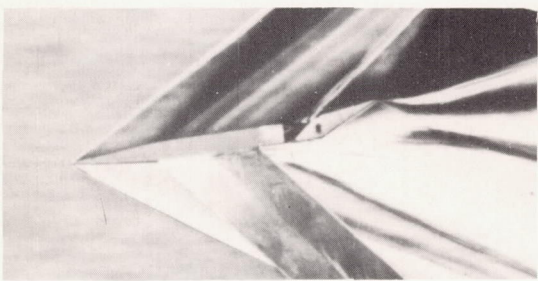




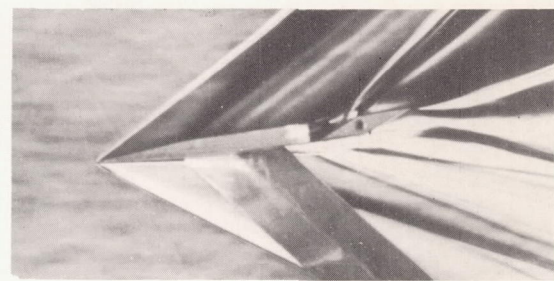
$$\alpha = -8^\circ, \delta = 0^\circ$$



$$\alpha = -8^\circ, \delta = 0^\circ$$



$$\alpha = -8^\circ, \delta = -18^\circ$$



$$\alpha = -8^\circ, \delta = -11^\circ$$



$$\alpha = -8^\circ, \delta = -30^\circ$$

$$\frac{c_b}{c_f} = 0.38$$



$$\alpha = -8^\circ, \delta = -25^\circ$$

$$\frac{c_b}{c_f} = 0.82$$

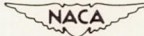
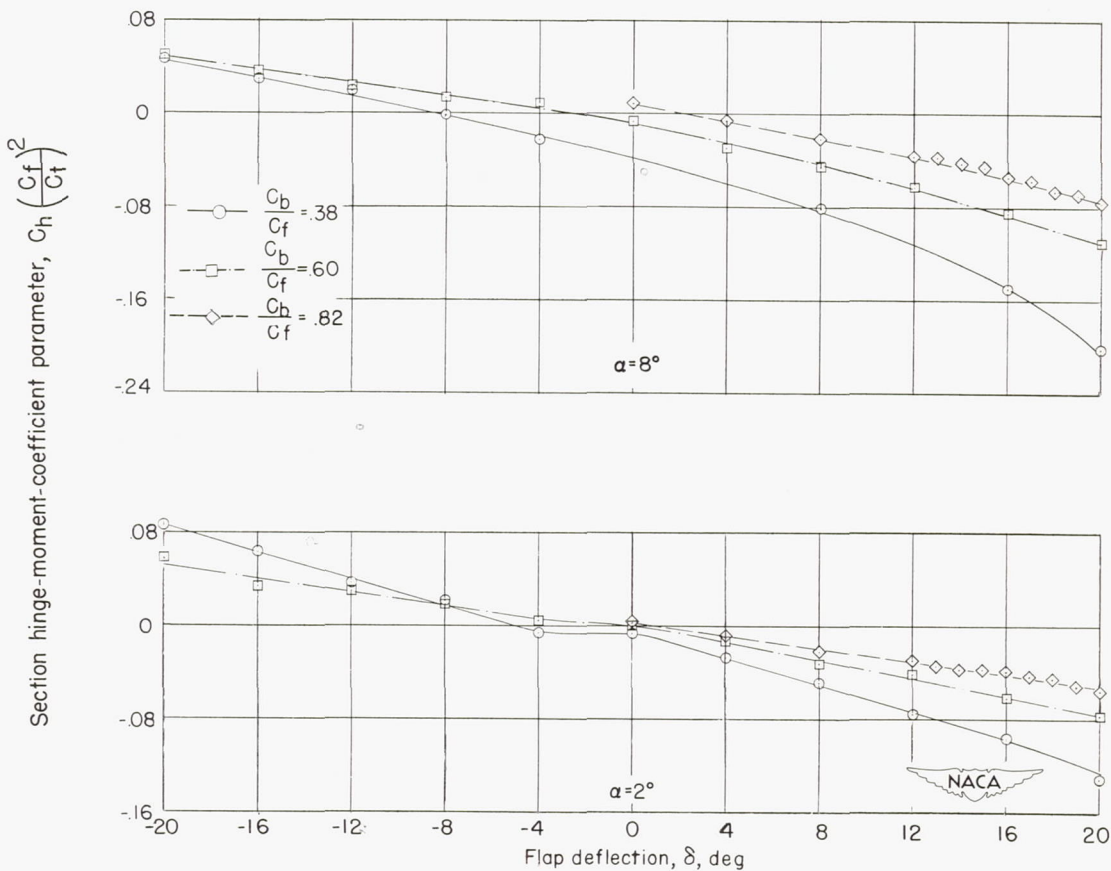
  
L-75141

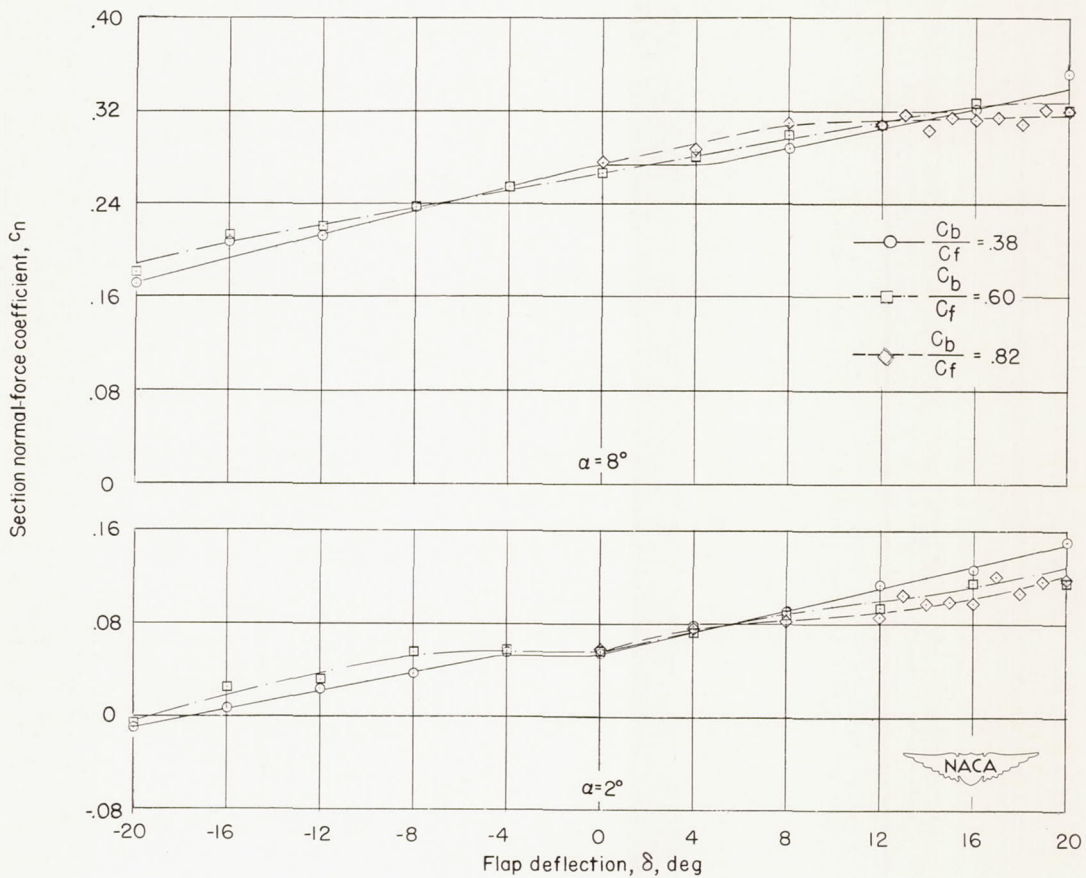
Figure 5.- Concluded.



$$(a) \quad c_h \left( \frac{c_f}{c_t} \right)^2$$

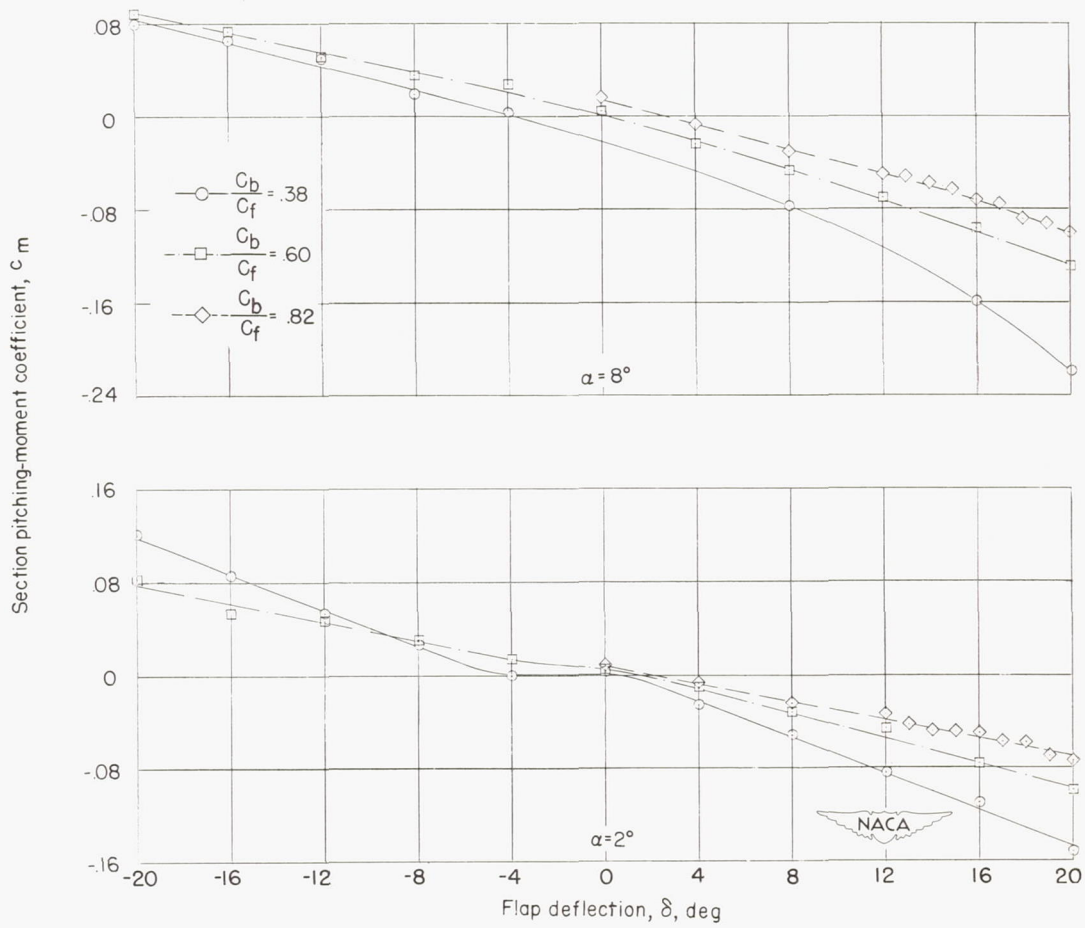
Figure 6.- Variation of section force and moment coefficients with flap deflection on a 6-percent-thick symmetrical wing equipped with trailing-edge flaps having various amounts of aerodynamic balance.  $M = 2.40$ ; wing-flap gap,  $0.033c$ ;  $R = 0.78 \times 10^6$ .





(b)  $c_n$ .

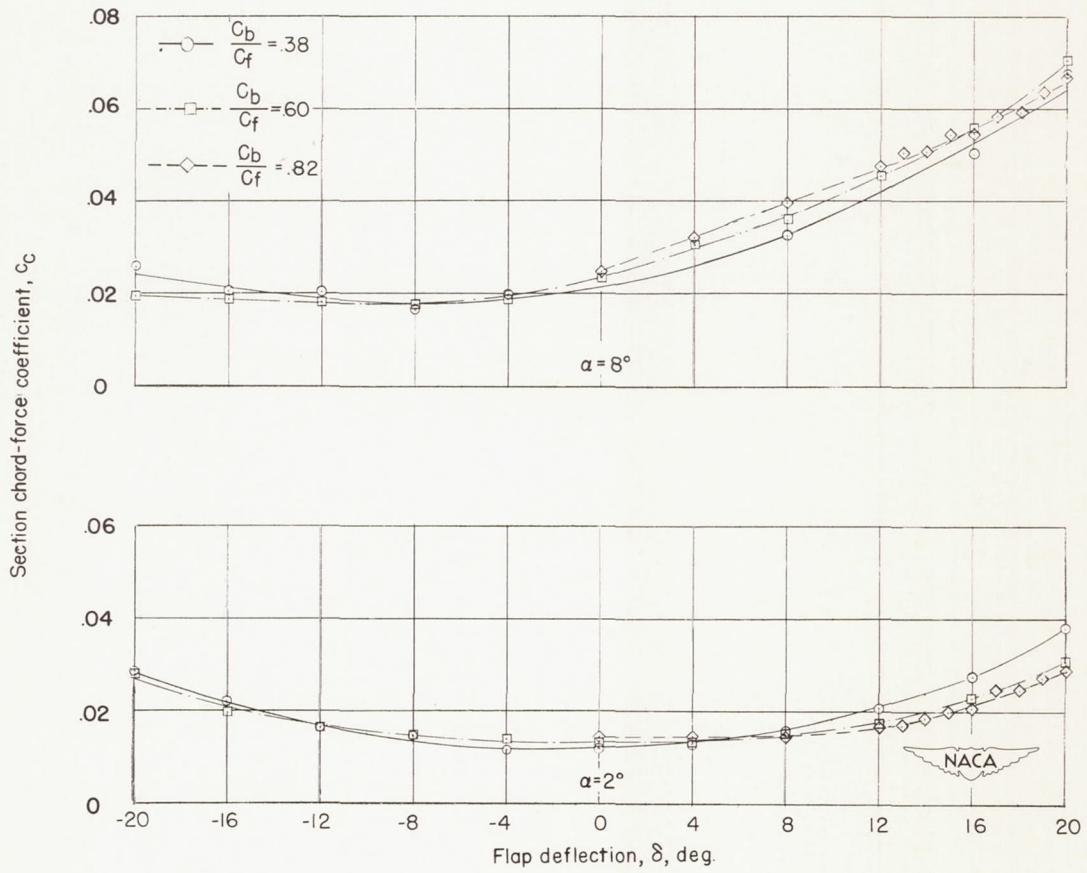
Figure 6.- Continued.



(c)  $c_m$ .

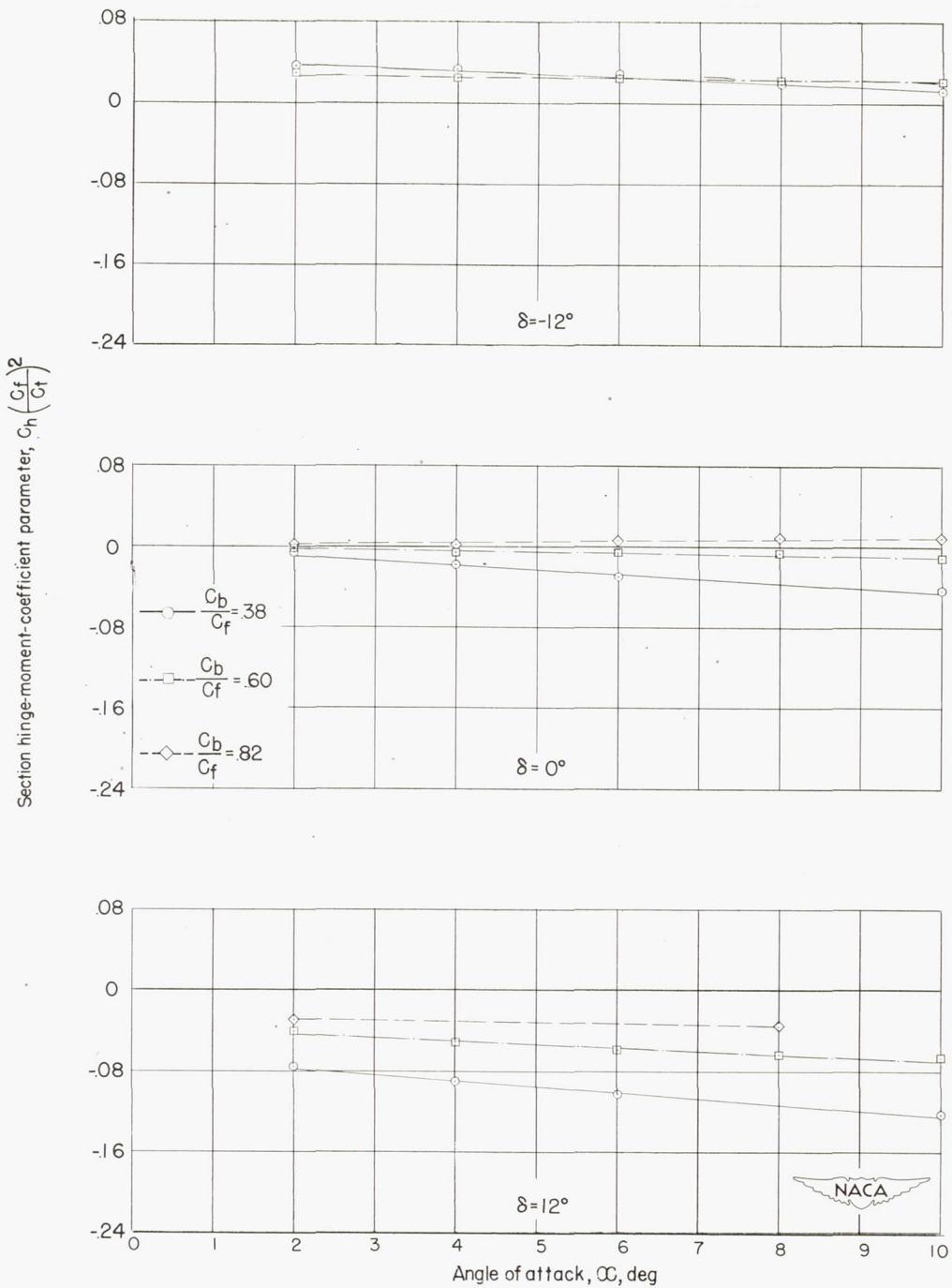
Figure 6.- Continued.





(d)  $c_c$ .

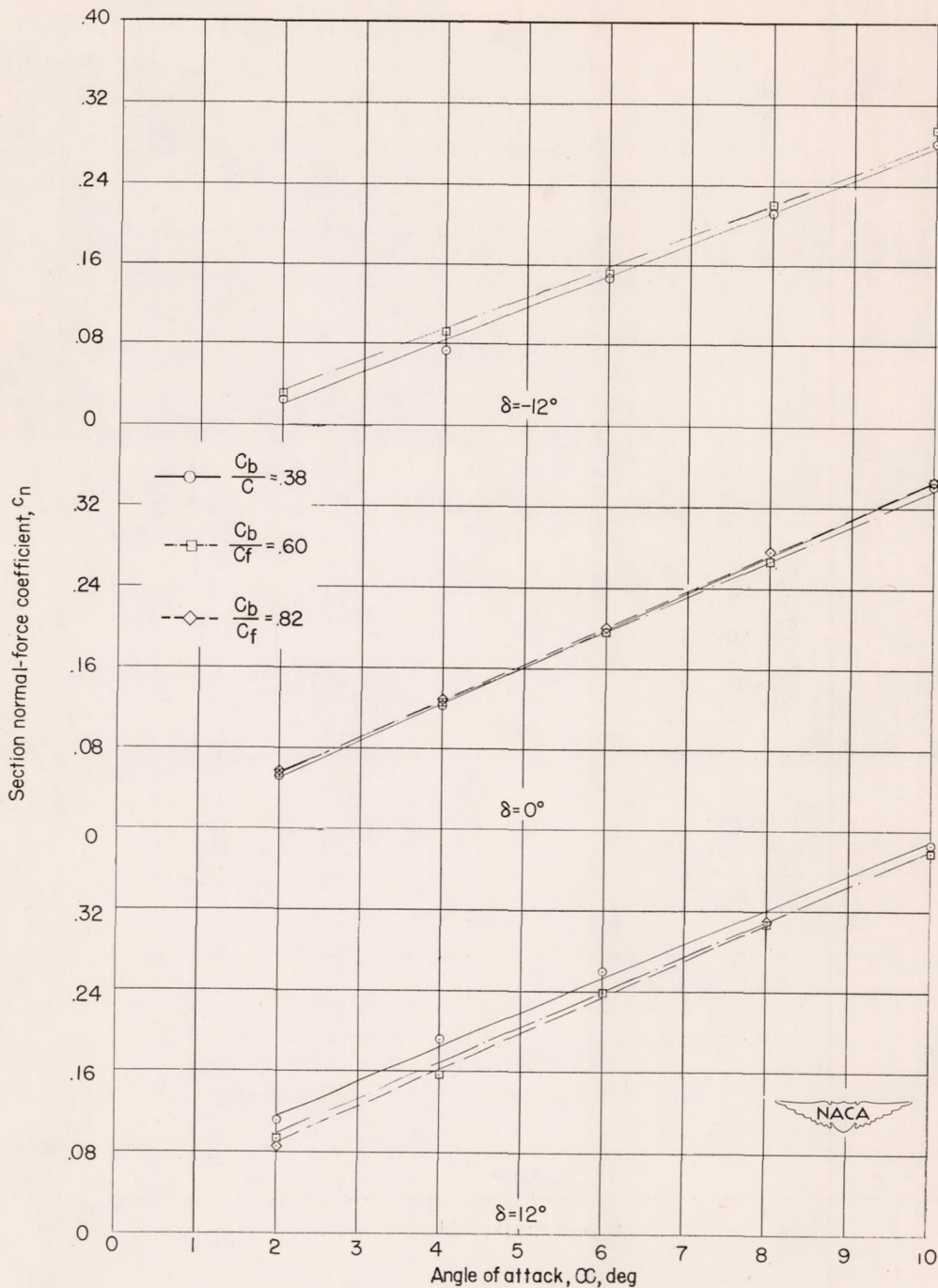
Figure 6.- Concluded.



$$(a) \quad c_h \left(\frac{c_f}{c_t}\right)^2$$

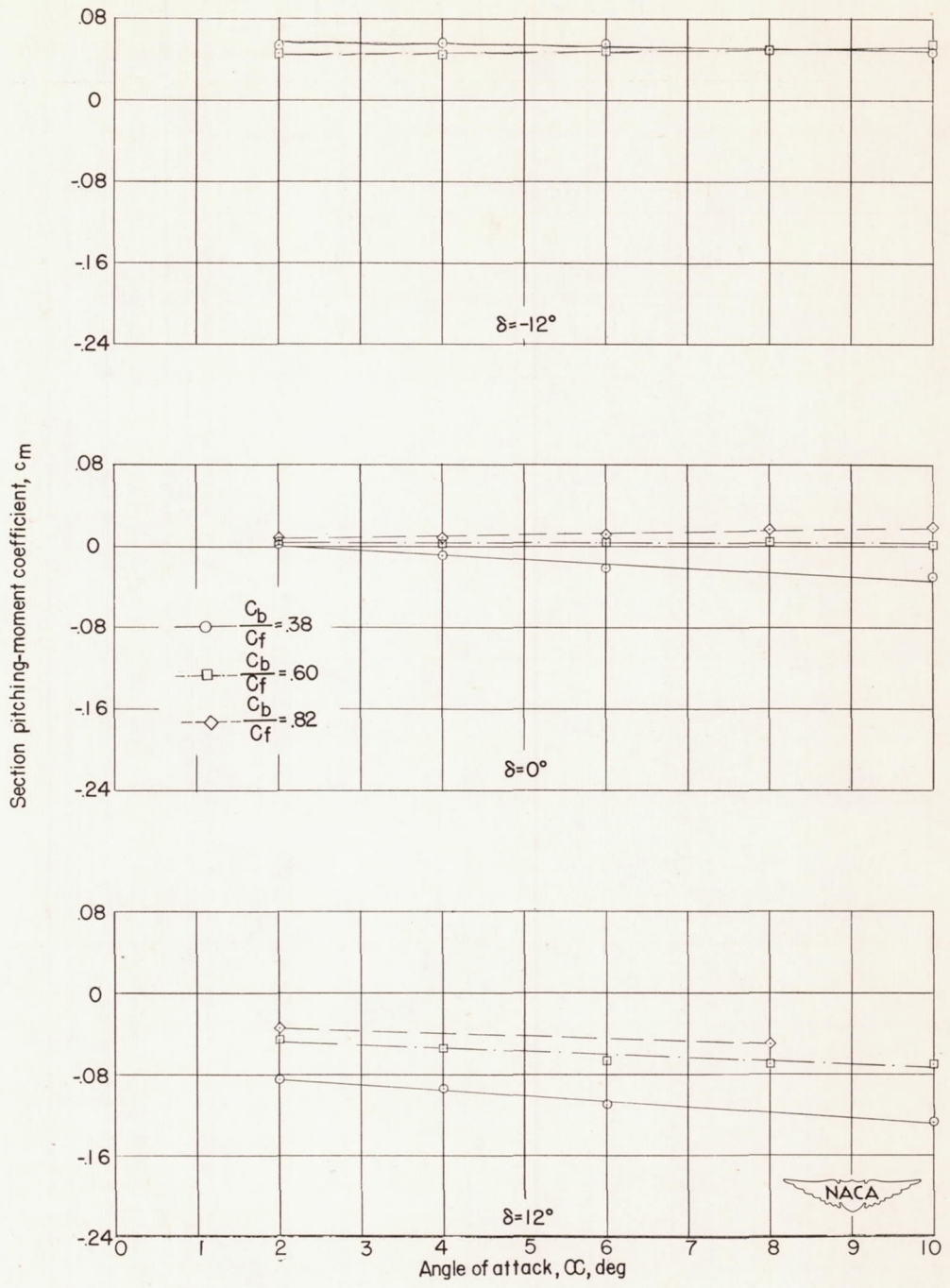
Figure 7.- Variation of section force and moment coefficients with angle of attack on a 6-percent-thick symmetrical wing equipped with trailing-edge flaps having various amounts of aerodynamic balance.  $M = 2.40$ ; wing-flap gap,  $0.033c$ ;  $R = 0.73 \times 10^6$ .





(b)  $c_n$ .

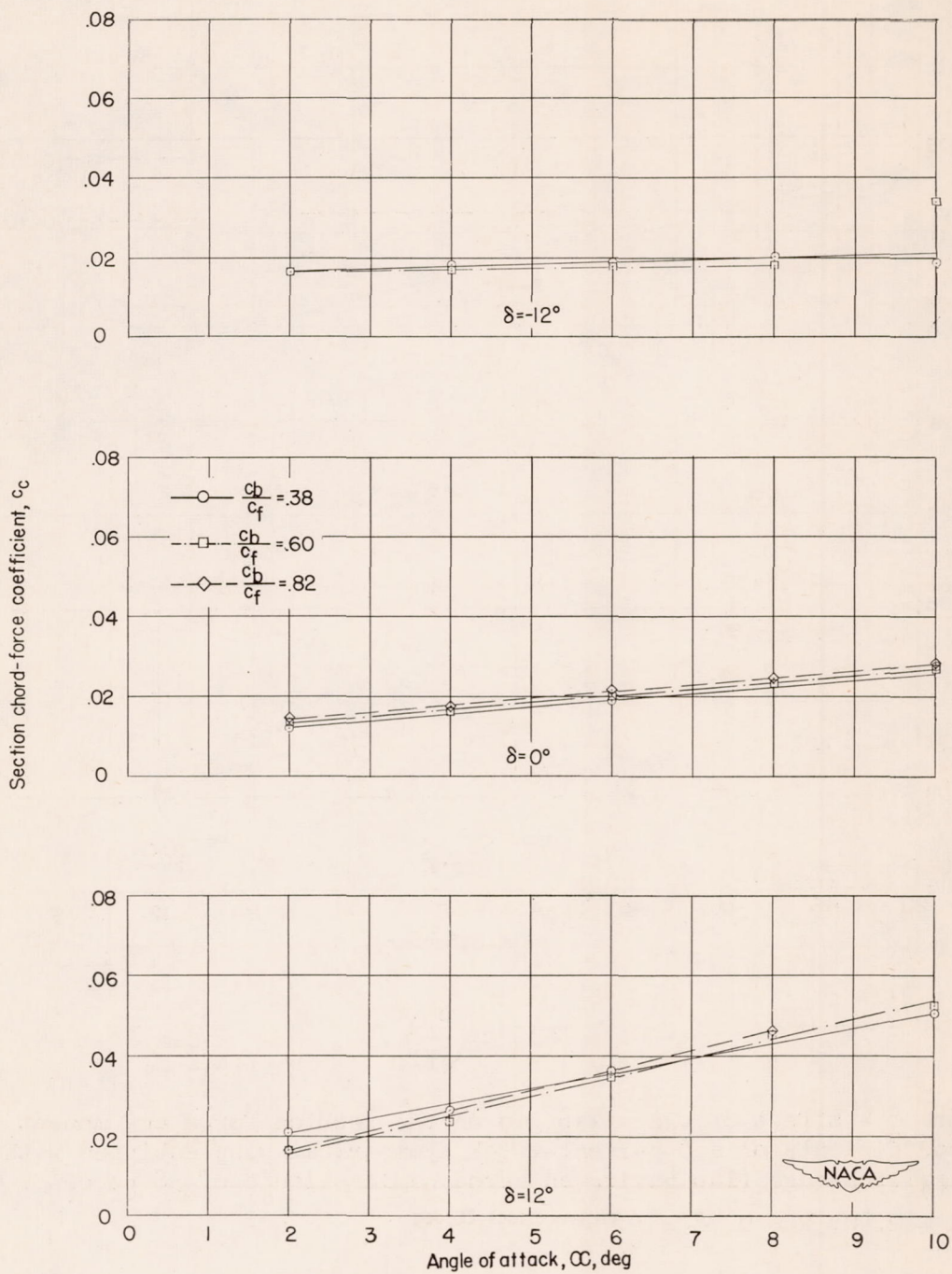
Figure 7.- Continued.



(c)  $c_m$ .

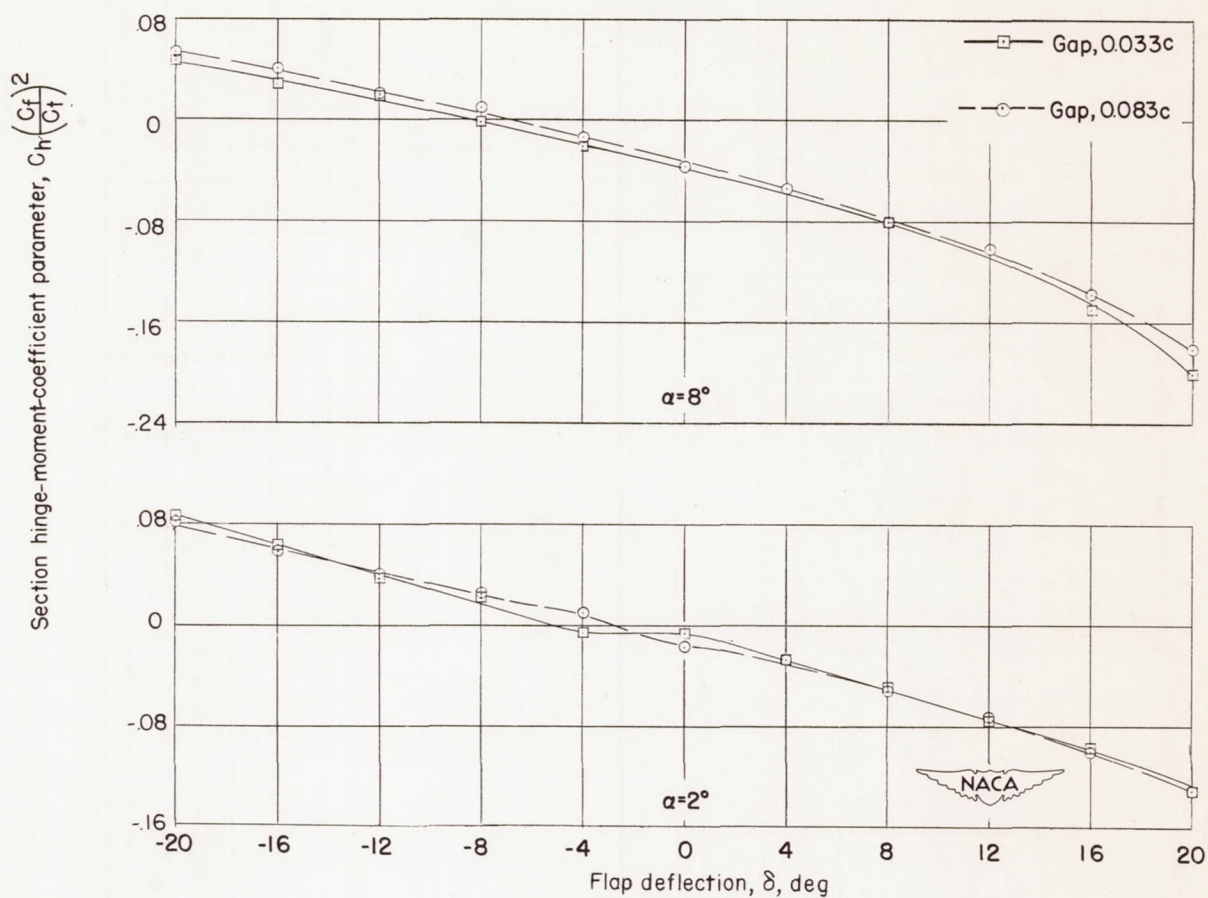
Figure 7.- Continued.





(d)  $c_c$ .

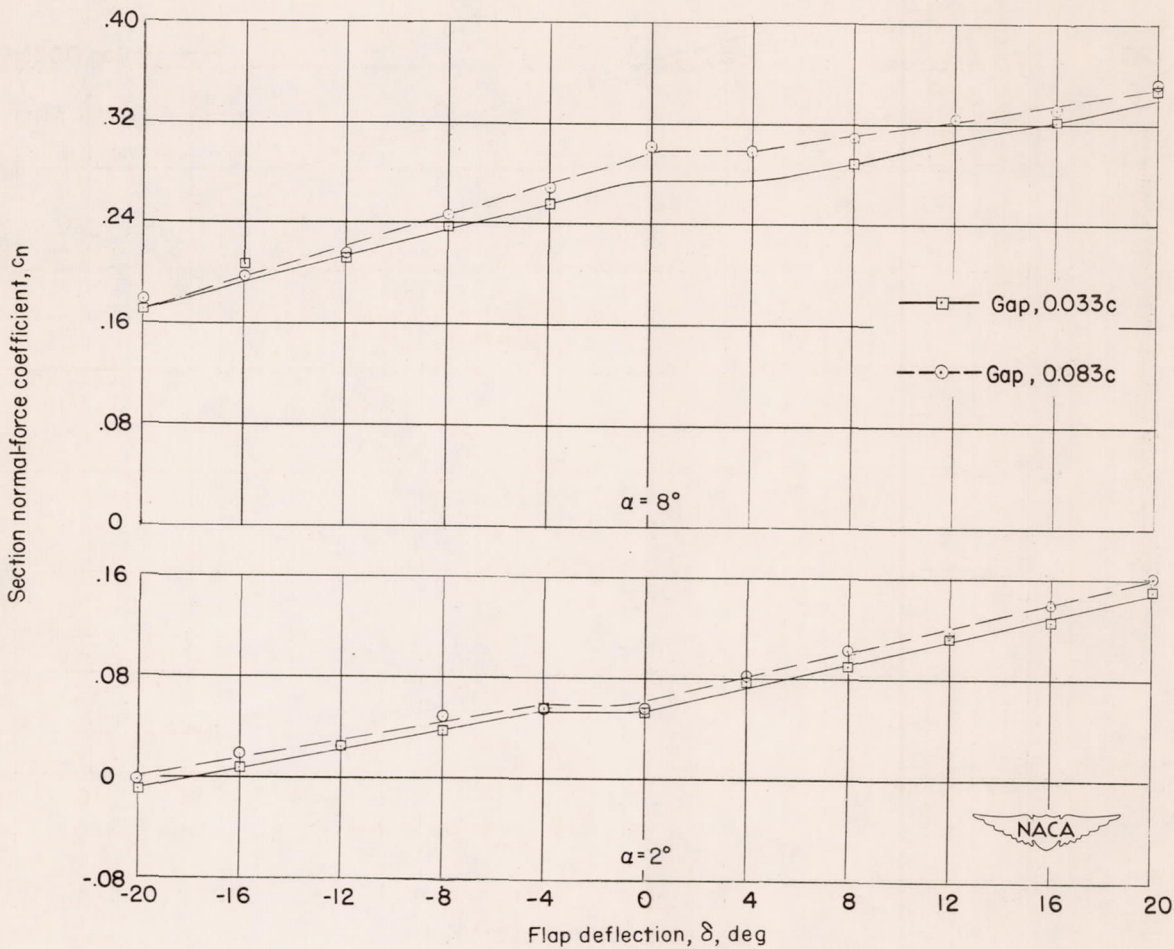
Figure 7.- Concluded.



$$(a) \quad c_h \left( \frac{c_f}{c_t} \right)^2.$$

Figure 8.- Effect of wing-flap gap on the section force and moment coefficients of a 6-percent-thick symmetrical wing equipped with a trailing-edge flap having an aerodynamic balance of 38 percent.

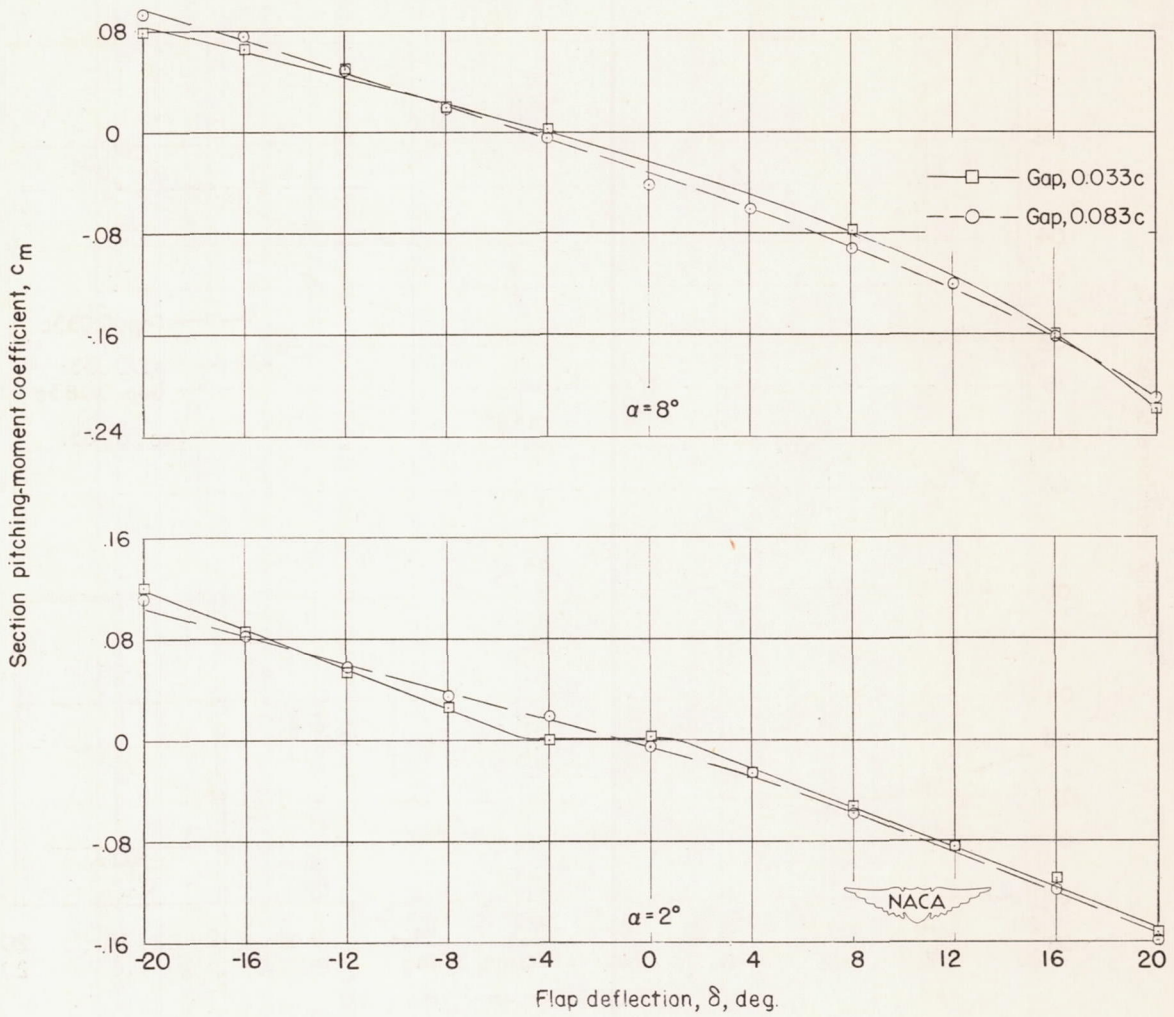
$$M = 2.40; R = 0.78 \times 10^6.$$



(b)  $c_n$ .

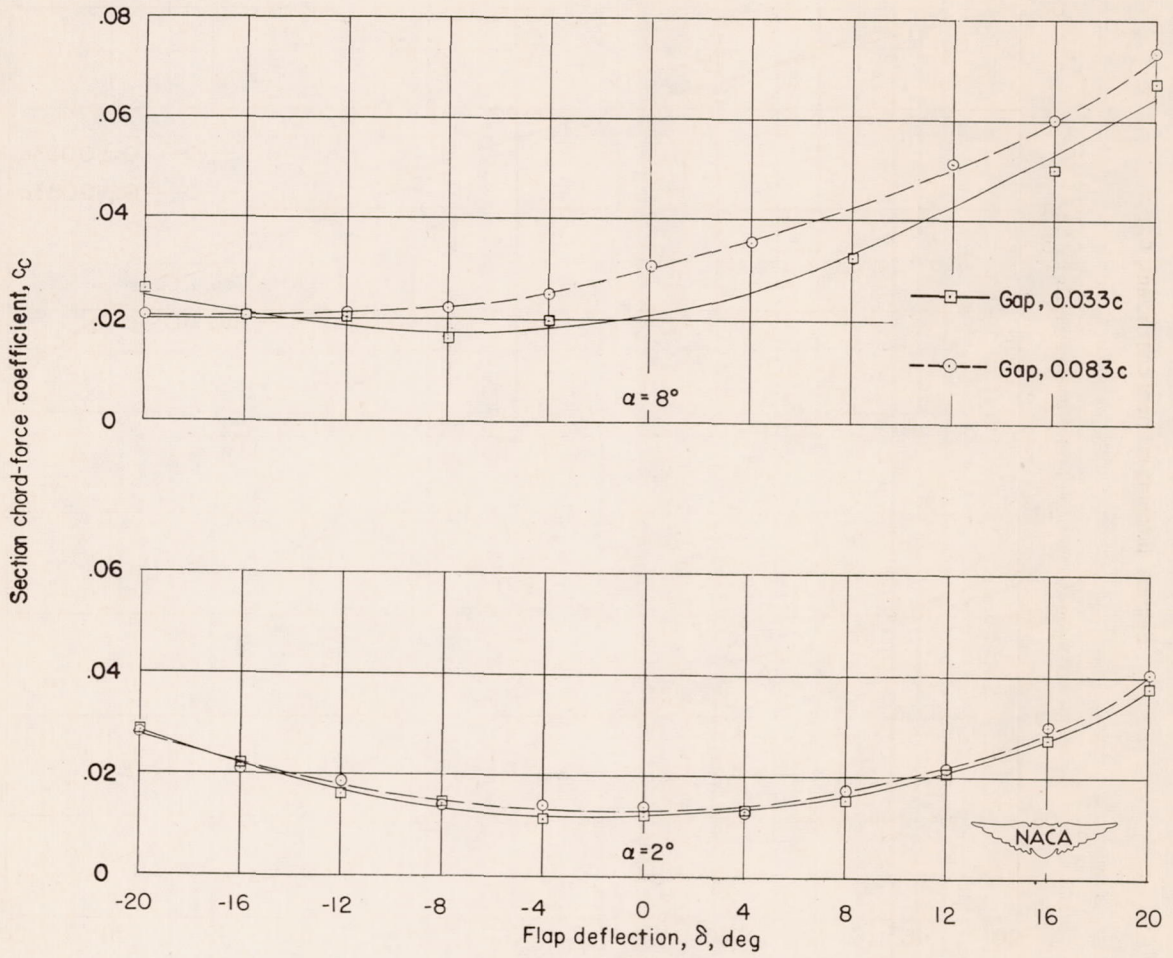
Figure 8.- Continued.





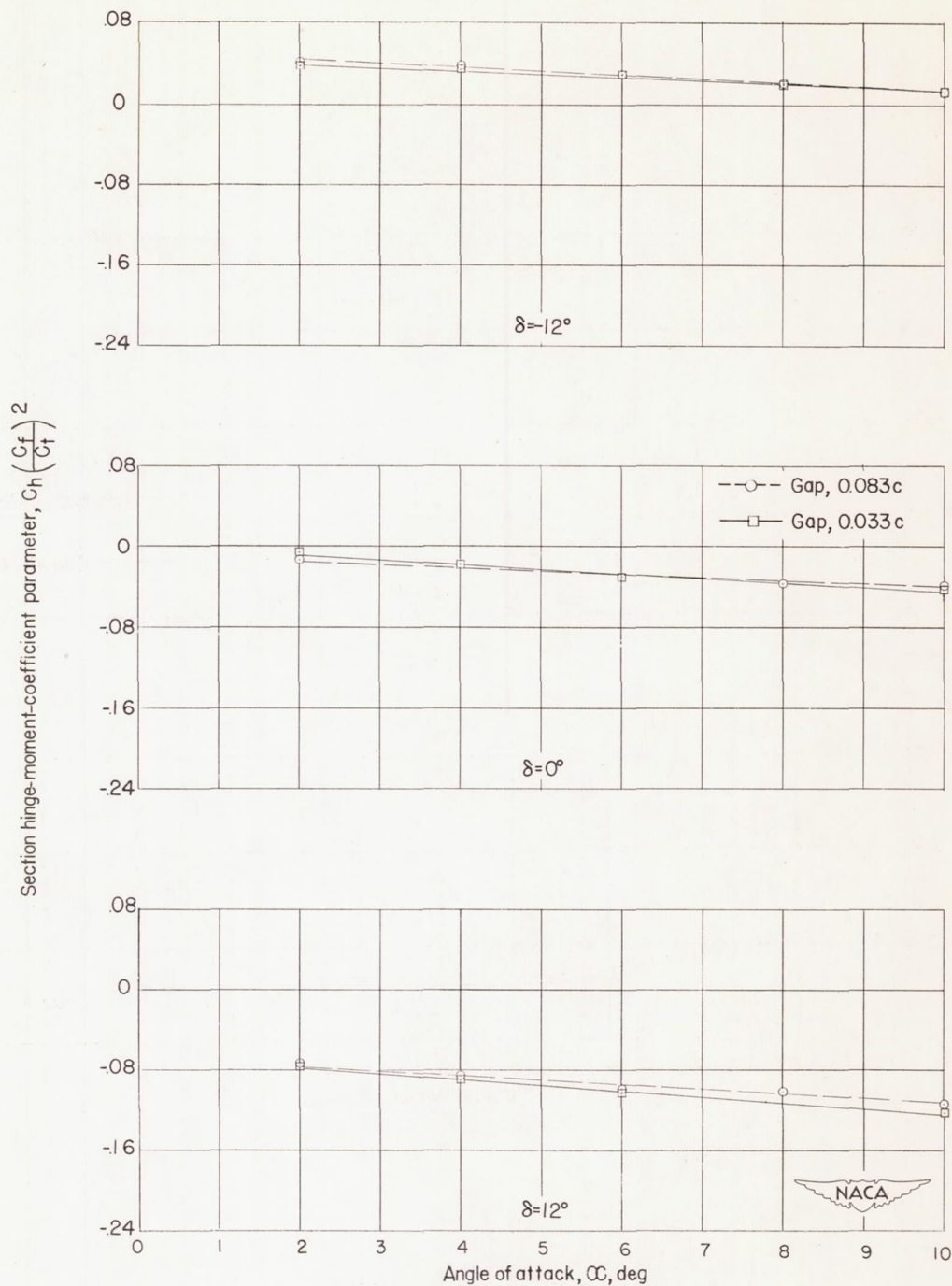
(c)  $c_m$ .

Figure 8.- Continued.



(d)  $c_c$ .

Figure 8.- Concluded.

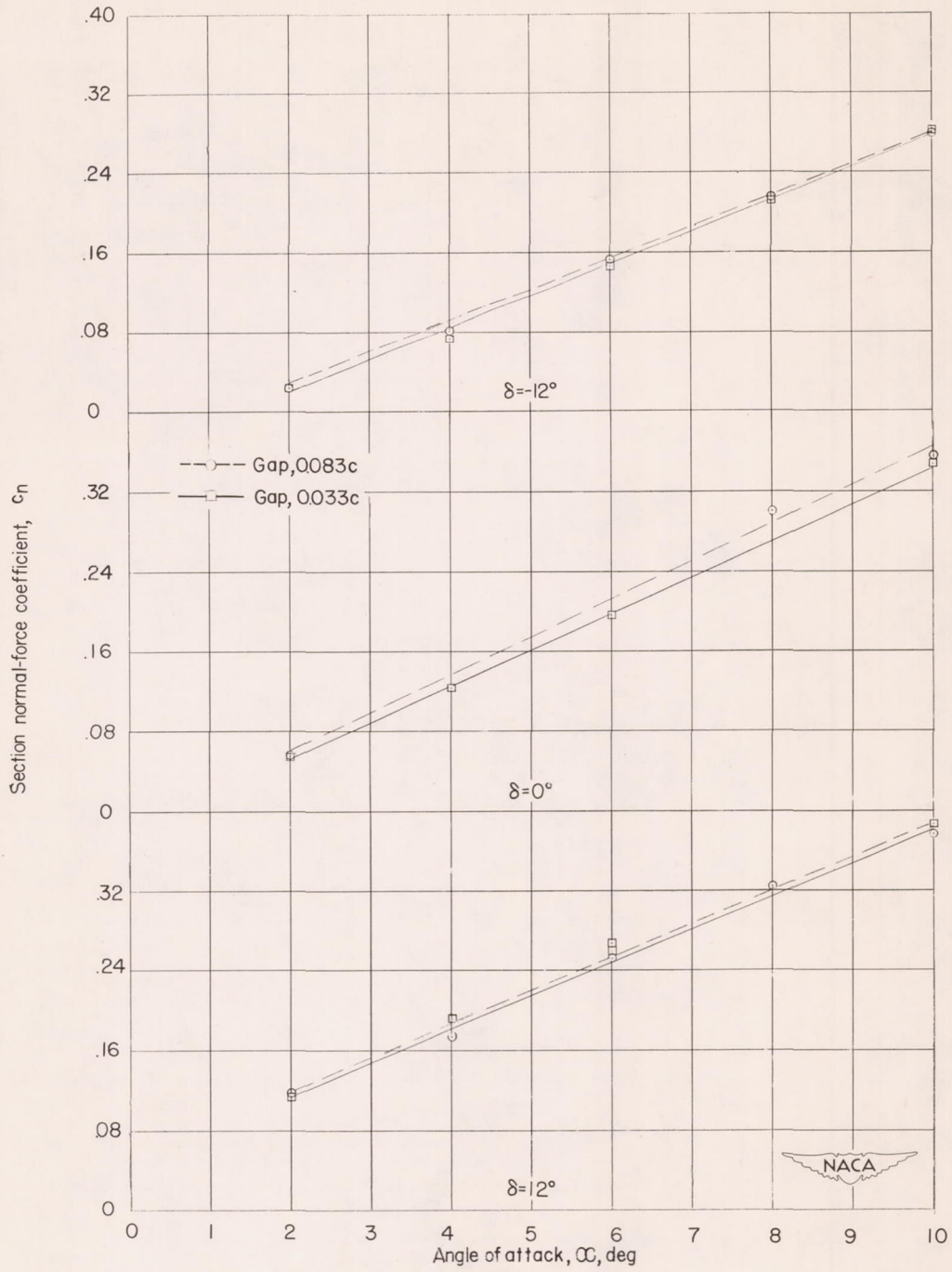


(a)  $C_h \left( \frac{C_f}{C_t} \right)^2$ .

Figure 9.- Effect of wing-flap gap on the section force and moment coefficients of a 6-percent-thick symmetrical wing equipped with a trailing-edge flap having an aerodynamic balance of 38 percent.

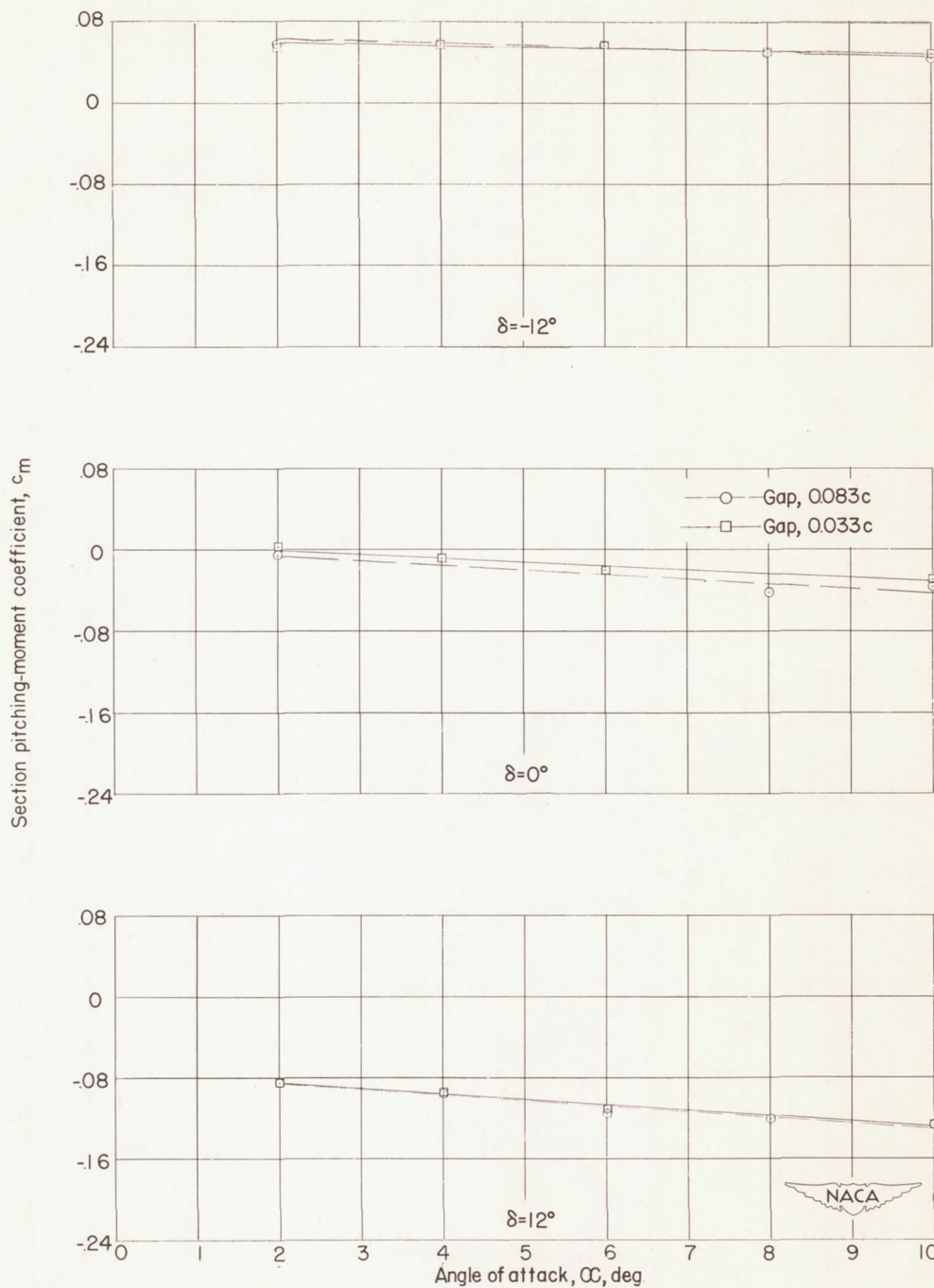
$M = 2.40$ ;  $R = 0.78 \times 10^6$ .





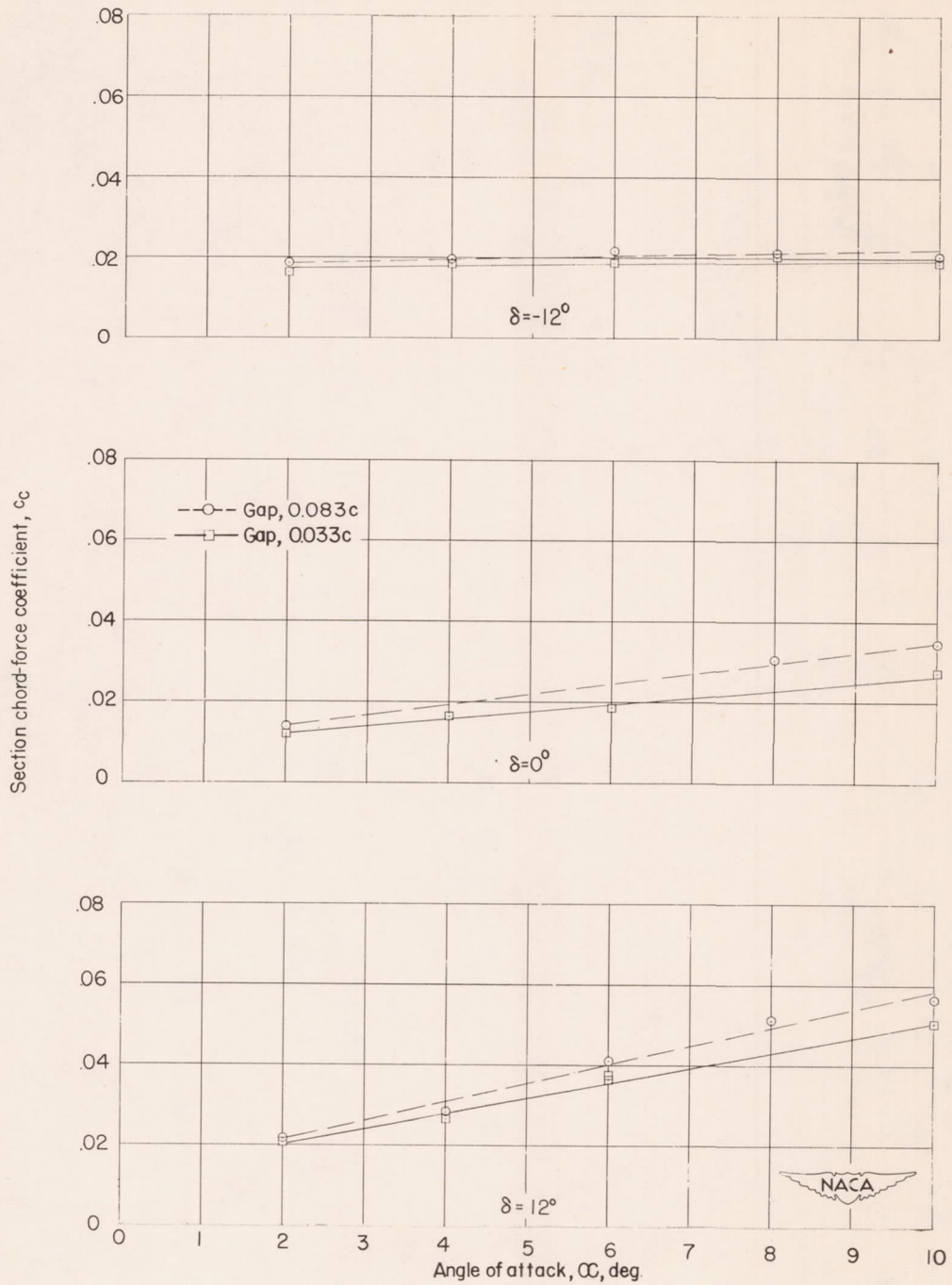
(b)  $c_n$ .

Figure 9.- Continued.



(c)  $c_m$ .

Figure 9.- Continued.



(d)  $c_c$ .

Figure 9.- Concluded.